



# Balancing Trained Immunity with Persistent Immune Activation and the Risk of Simian Immunodeficiency Virus Infection in Infant Macaques Vaccinated with Attenuated *Mycobacterium tuberculosis* or *Mycobacterium bovis* BCG Vaccine

Kara Jensen,<sup>a</sup> Myra Grace dela Pena-Ponce,<sup>a</sup> Michael Piatak, Jr.,<sup>b,†</sup> Rebecca Shoemaker,<sup>b</sup> Kelli Oswald,<sup>b</sup> William R. Jacobs, Jr.,<sup>c</sup> Glenn Fennelly,<sup>d</sup> Carissa Lucero,<sup>b</sup> Katie R. Mollan,<sup>e</sup> Michael G. Hudgens,<sup>f</sup> Angela Amedee,<sup>g</sup> Pamela A. Kozlowski,<sup>g</sup> Jacob D. Estes,<sup>b</sup> Jeffrey D. Lifson,<sup>b</sup> Koen K. A. Van Rompay,<sup>h</sup> Michelle Larsen,<sup>c</sup> Kristina De Paris<sup>a</sup>

Department of Microbiology and Immunology and Center for AIDS Research, School of Medicine, University of North Carolina, Chapel Hill, North Carolina, USA<sup>a</sup>; AIDS and Cancer Virus Program, Leidos Biomedical Research, Inc., Frederick National Laboratory for Cancer Research, Frederick, Maryland, USA<sup>b</sup>; Albert Einstein College of Medicine, New York, New York, USA<sup>c</sup>; Rutgers New Jersey Medical School, Newark, New Jersey, USA<sup>d</sup>; Lineberger Cancer Center and Center for AIDS Research, University of North Carolina, Chapel Hill, North Carolina, USA<sup>e</sup>; Gillings School of Global Public Health and Center for AIDS Research, University of North Carolina, Chapel Hill, North Carolina, USA<sup>f</sup>; Department of Microbiology, Immunology, and Parasitology, Louisiana State University Health Sciences Center, New Orleans, Louisiana, USA<sup>g</sup>; California National Primate Research Center, University of California, Davis, Davis, California, USA<sup>h</sup>

**ABSTRACT** Our goal is to develop a pediatric combination vaccine to protect the vulnerable infant population against human immunodeficiency virus type 1 (HIV-1) and tuberculosis (TB) infections. The vaccine consists of an auxotroph *Mycobacterium tuberculosis* strain that coexpresses HIV antigens. Utilizing an infant rhesus macaque model, we have previously shown that this attenuated *M. tuberculosis* (*AMtb*)-simian immunodeficiency virus (SIV) vaccine is immunogenic, and although the vaccine did not prevent oral SIV infection, a subset of vaccinated animals was able to partially control virus replication. However, unexpectedly, vaccinated infants required fewer SIV exposures to become infected compared to naive controls. Considering that the current TB vaccine, *Mycobacterium bovis* bacillus Calmette-Guérin (BCG), can induce potent innate immune responses and confer pathogen-unspecific trained immunity, we hypothesized that an imbalance between enhanced myeloid cell function and immune activation might have influenced the outcome of oral SIV challenge in *AMtb*-SIV-vaccinated infants. To address this question, we used archived samples from unchallenged animals from our previous *AMtb*-SIV vaccine studies and vaccinated additional infant macaques with BCG or *AMtb* only. Our results show that vaccinated infants, regardless of vaccine strain or regimen, had enhanced myeloid cell responses. However, CD4<sup>+</sup> T cells were concurrently activated, and the persistence of these activated target cells in oral and/or gastrointestinal tissues may have facilitated oral SIV infection. Immune activation was more pronounced in BCG-vaccinated infant macaques than in *AMtb*-vaccinated infant macaques, indicating a role for vaccine attenuation. These findings underline the importance of understanding the interplay of vaccine-induced immunity and immune activation and its effect on HIV acquisition risk and outcome in infants.

Received 11 July 2016 Returned for modification 29 July 2016 Accepted 12 September 2016

Accepted manuscript posted online 21 September 2016

**Citation** Jensen K, dela Pena-Ponce MG, Piatak M, Jr, Shoemaker R, Oswald K, Jacobs WR, Jr, Fennelly G, Lucero C, Mollan KR, Hudgens MG, Amedee A, Kozlowski PA, Estes JD, Lifson JD, Van Rompay KKA, Larsen M, De Paris K. 2017. Balancing trained immunity with persistent immune activation and the risk of simian immunodeficiency virus infection in infant macaques vaccinated with attenuated *Mycobacterium tuberculosis* or *Mycobacterium bovis* BCG vaccine. *Clin Vaccine Immunol* 24: e00360-16. <https://doi.org/10.1128/CLI.00360-16>.

**Editor** Helene F. Rosenberg, IIS/LAD/NIAID/NIH

**Copyright** © 2017 American Society for Microbiology. All Rights Reserved.

Address correspondence to Kristina De Paris, [abelk@med.unc.edu](mailto:abelk@med.unc.edu).

† Deceased.

For a commentary on this article, see <https://doi.org/10.1128/CLI.00509-16>.

**KEYWORDS** pediatric HIV/SIV, vaccine, immune activation, myeloid cells

Human immunodeficiency virus (HIV) and tuberculosis (TB) infections remain highly prevalent in many parts of the world and often show substantial geographical overlap. Infants represent one of the populations most vulnerable to both diseases. An HIV vaccine is not yet available, and although a vaccine to prevent TB infection, the live attenuated *Mycobacterium bovis* bacillus Calmette-Guérin (BCG) vaccine, is routinely administered to >80% of neonates globally and is effective at preventing the most severe complications of TB, BCG efficacy wanes with age (1–3). In HIV-infected infants and infants at risk for HIV, the BCG vaccine is contraindicated due to the potential of inducing disseminated BCG disease (4). Thus, both a new TB vaccine and a pediatric HIV vaccine are urgently needed to reduce infant mortality and morbidity in areas of high HIV and TB prevalence. Toward this goal, we aimed to develop a pediatric combination HIV-TB vaccine that could protect infants against HIV and TB infections. Our vaccine was intentionally designed to retain the immunogenicity of BCG but was more attenuated to exhibit an improved safety profile, while expressing HIV antigens to induce both HIV-specific and TB-specific immune responses. Further, we opted to utilize an attenuated human-adapted *Mycobacterium tuberculosis* for improved immune memory, rather than further edit the *M. bovis* backbone of BCG.

Our pediatric TB-HIV combination vaccine is based on an auxotroph mutant of *Mycobacterium tuberculosis* that has deletions in the *panCD*, *leuCD*, and *secA2* loci that render this attenuated *M. tuberculosis* (*AMtb*) strain mc<sup>2</sup>6208 replication incompetent (5–7). In fact, because these bacteria are unable to synthesize essential nutrients (panthothenate and leucine), replication in unsupplemented conditions, such as a mammalian host, can occur only temporarily until the cell reserves are depleted. In contrast, BCG does not harbor auxotroph mutations and can replicate freely until thwarted by the host immune system. Using experimental simian immunodeficiency virus (SIV) infection of infant rhesus macaques, an animal model of pediatric HIV infection, we have previously demonstrated that this *AMtb* vaccine, in contrast to BCG, does not cause mycobacterial dissemination or TB tissue pathology (8). Further modification of the mc<sup>2</sup>6208 vaccine strain to coexpress SIVgag (mc<sup>2</sup>6435) or SIVenv (mc<sup>2</sup>6439) rendered this vaccine capable of inducing both TB- and SIV-specific T cell and antibody responses in infant macaques (9, 10). Although these vaccine-induced SIV-specific immune responses were not sufficient to prevent oral SIV acquisition, a subset of vaccinated infant macaques with higher-avidity plasma SIV Env-specific IgG antibodies and SIV Env-specific mucosal IgA antibodies showed better control of SIV replication upon infection (9). At the same time, unexpectedly, the group of vaccinated infant macaques had a twofold-higher SIV infection risk per exposure compared to unvaccinated infants (9). Despite not being statistically significant, the difference in the per exposure risk of SIV infection was reminiscent of increased CD4<sup>+</sup> T cell activation, and thereby a potentially increased risk of HIV infection, seen in South African infants after BCG vaccination (11, 12).

In human neonates, a single immunization with BCG at birth has been shown to be highly immunogenic despite the infant's reduced ability to mount potent T helper 1 (Th1) responses. Further, the introduction of the BCG vaccine has been associated with a significant drop in overall childhood mortality. In addition to protection against TB, inherent adjuvant properties of BCG can improve immunological responses to other neonatal vaccines (13, 14). Only recently have we begun to understand the mechanism(s) by which BCG can exert these beneficial effects. Studies in human adults have shown that BCG vaccination induces epigenetic modifications in monocytes that can persist for several months, resulting in improved functional capacity and higher responses to both *M. tuberculosis* and unrelated antigens (15). This phenomenon, which has been characterized as an aspect of "trained immunity," was not restricted to monocytes and macrophages that are the target cells for mycobacteria but was also extended to T cells (16). Therefore, it has been proposed that novel TB vaccine

candidates should aim to preserve these unique features of BCG. In fact, among the new TB vaccine candidates under development, several are based on additional attenuations of *M. bovis* within the existing BCG vaccine or on attenuated *M. tuberculosis* strains similar to the auxotroph *AMtb* vaccines used here (17–21). Recombinant BCG strains expressing HIV antigens are also in development as potential HIV vaccines and have been tested in mice (22–24) and in adult (25–29) and neonatal (30) macaques. Considering the high risk of HIV and TB infection in infants, especially in sub-Saharan Africa, we deemed it important to understand how novel TB vaccines or combination HIV-TB vaccines might impact HIV acquisition.

In a first attempt to better define the beneficial effects of mycobacterial vaccines and to weigh them against potentially negative outcomes on infant HIV infection risk, we report here studies conducted on archived tissue samples from animals immunized with the *AMtb*-SIV prime/modified vaccinia Ankara (MVA)-SIV boost regimen that were not challenged with SIV (10) or samples from animals included in our recent efficacy studies that were collected prior to or at the time of the first SIV challenge (9). To exclude any effects of the vaccine booster component or the SIV inserts on oral SIV acquisition, we expanded upon those historical studies by vaccinating infant macaques with *AMtb* vaccines only (*AMtb*-SIV prime plus a homologous boost) or animals primed only with *AMtb*-SIV, the *AMtb* strain without SIV cassettes, or the human infant regimen of BCG. Specifically, the current study examined the potential of our *AMtb* vaccine to increase functional responses of infant monocytes/macrophages and whether enhanced myeloid cell function was associated with immune activation that could potentially predispose infants to SIV infection.

## RESULTS

**Increased functional responses in myeloid cell population of *AMtb*-vaccinated infant macaques.** In human adults, the persistence of heightened monocyte function has been described as a hallmark of BCG-induced trained immunity (15, 31, 32). To determine whether our *AMtb* vaccine mc<sup>2</sup>6435 (expressing SIVgag) could also enhance monocyte responses and whether it could do so in the pediatric setting, we utilized archived peripheral blood mononuclear cell (PBMC) and tissue samples from SIV-uninfected infant macaques that were vaccinated with strain mc<sup>2</sup>6435 at birth, boosted with MVA-SIV at 3 and 6 weeks of age, and monitored for 16 to 18 weeks to determine vaccine-induced SIV- and TB-specific immune responses in blood and tissues (10). As mycobacteria infect not only monocytes/macrophages but also dendritic cells (DC), we tested both monocytes/macrophages and myeloid DC (mDC) for their ability to produce cytokines in response to Toll-like receptor (TLR) ligation. Although mycobacteria are not known to signal through Toll-like receptor 7 (TLR7) or TLR8, we chose the TLR7/8 agonist R848 because monocytes/macrophages and myeloid dendritic cells from infants show reduced function compared to those from adults, and R848 has been demonstrated to potently activate infant cell populations (33, 34). At 16 to 18 weeks after vaccination, *in vitro* R848 stimulation of PBMC resulted in higher frequencies of interleukin 12 (IL-12)-producing monocytes/macrophages (Fig. 1A) and mDC (Fig. 1B) in vaccinated animals than in naive control animals, but these differences were not statistically significant. Peripheral blood monocytes/macrophages of *AMtb*-vaccinated infant macaques did, however, express increased levels of the activation markers CCR5 (chemokine [C-C motif] receptor 5) and CD69 compared to naive controls (Fig. 1C). In contrast to PBMC, tissue analyses revealed clear differences in the functional capacity of myeloid cell populations from *AMtb*-vaccinated and unvaccinated infant macaques. It is particularly noteworthy that greater frequencies of IL-12- or tumor necrosis factor alpha (TNF- $\alpha$ )-producing monocytes/macrophages (Fig. 1D) and mDC (Fig. 1E) were observed in the tonsils and submandibular lymph nodes (LN) of *AMtb*-vaccinated animals compared to naive controls. These results indicated that a single oral administration of an *AMtb* vaccine during the first week of life could enhance the function of infant monocytes/macrophages and mDC and that these responses persisted for at least 16 to 18 weeks in blood and tissues of infant macaques. As oral and intestinal

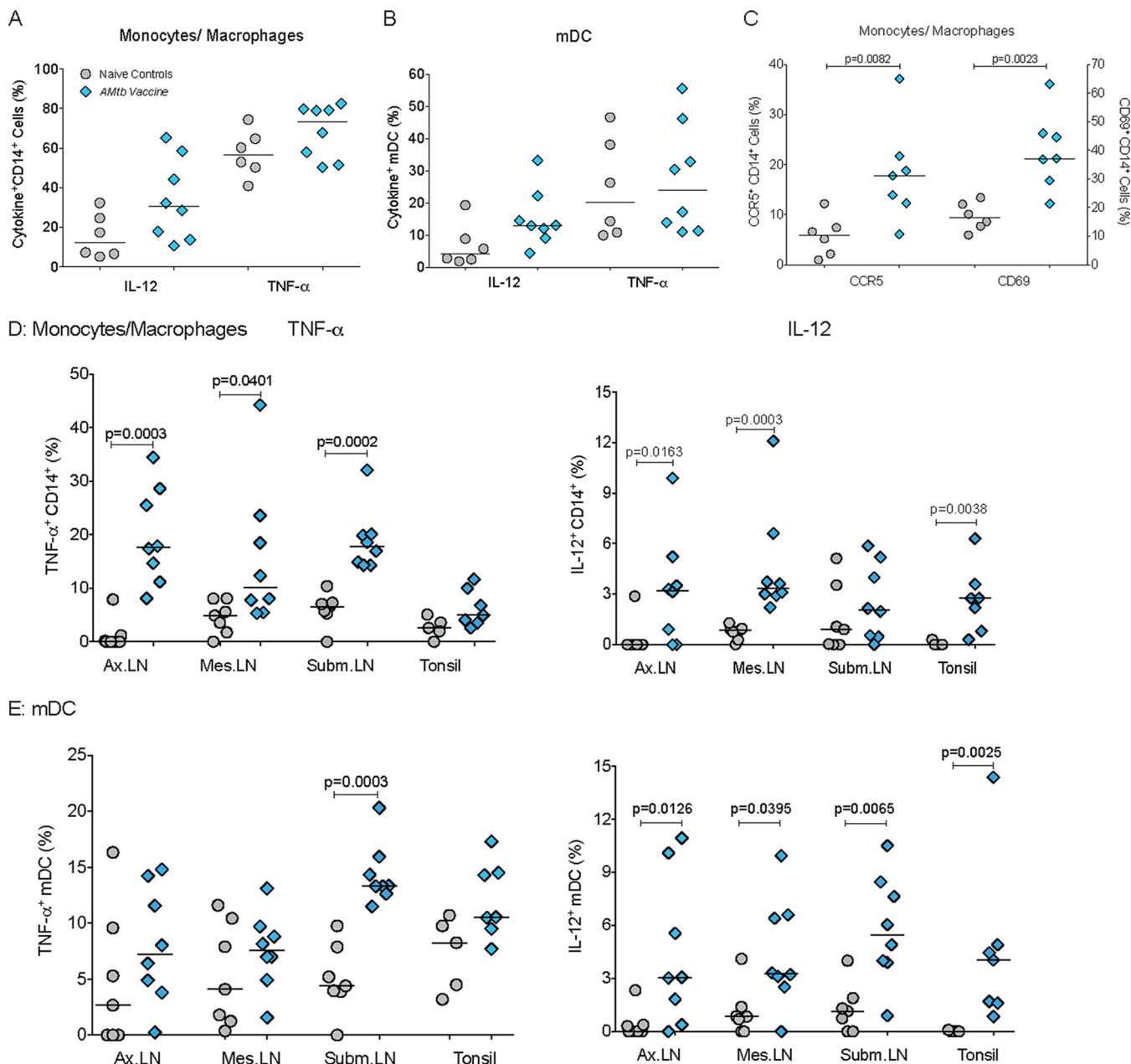


**FIG 1** Increased functional responsiveness of monocytes/macrophages and mDC. (A and B) Frequencies of IL-12- or TNF- $\alpha$ -producing monocytes/macrophages and mDC, respectively, in PBMC from naive controls and *AMtb*-vaccinated infant macaques at 16 to 18 weeks after vaccination. (C) Frequencies of CCR5<sup>+</sup> or CD69<sup>+</sup> peripheral blood monocytes/macrophages from the same animals. (D and E) Frequencies of TNF- $\alpha$ - or IL-12-producing monocytes/macrophages (D) and mDC (E) from the axillary (Ax.), mesenteric (Mes.), and submandibular (Subm.) lymph nodes (LN) and tonsils of vaccinated infant animals after *in vitro* stimulation with R848. Each symbol represents the value for an individual animal. The short horizontal bar in all graphs represents the median value for the group. Statistically significant differences between the groups are listed as P values and were determined by exact Mann-Whitney test.

tissues are presumed sites of entry and early SIV replication after oral exposure and our goal is to develop a pediatric HIV-TB combination vaccine, we deemed it important to test whether the *AMtb* vaccination had also resulted in CD4<sup>+</sup> T cell activation.

**Prolonged CD4<sup>+</sup> T cell activation after *AMtb* vaccination of infant macaques.**

Indeed, 16 to 18 weeks after vaccination with *AMtb*, the frequencies of CD4<sup>+</sup> CCR5<sup>+</sup> T cells were significantly higher in PBMC, retropharyngeal LN, and colons of *AMtb*-vaccinated animals than in naive controls (Fig. 2). In addition, frequencies of Ki-67<sup>+</sup>, PD-1<sup>+</sup>, and CD69<sup>+</sup> CD4<sup>+</sup> T cells were generally higher in retropharyngeal LN and colon cell suspensions of cells from *AMtb*-vaccinated infants than in those from naive controls

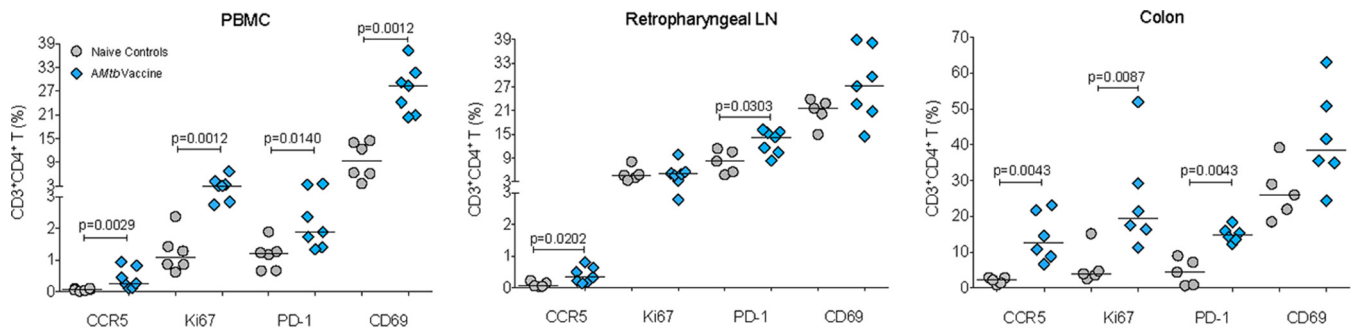


**FIG 2** CD4<sup>+</sup> T cell activation in tissues at 16 to 18 weeks after *AMtb* vaccination. Percentages of CCR5-, Ki67-, PD-1-, and CD69-positive CD4<sup>+</sup> T cells were measured by flow cytometric analysis in PBMC, retropharyngeal lymph nodes, and the colon at 16 to 18 weeks postvaccination. See the legend to Fig. 1.

(Fig. 2). Although only PBMC, retropharyngeal LN, and colons were available for this retroactive analysis, these data further confirmed that the *AMtb*-induced immune activation persisted for several weeks to months after vaccination and provided evidence that SIV target cell frequencies at presumed sites of viral entry and/or early replication were concurrently increased. These findings of persistent *AMtb* vaccine-induced immune activation in myeloid cell and CD4<sup>+</sup> T cell populations in blood and tissues reiterated the important question of whether vaccine-induced immune activation could enhance the risk for HIV/SIV infection, as suggested by the results of the STEP HIV vaccine trial (35–37).

**Study design to test the association between *AMtb* or BCG vaccines and oral SIV challenge outcome.** We recently reported that an *AMtb*-SIV prime/MVA-SIV boost regimen did not protect infant macaques against oral SIV infection; furthermore, vaccinated animals appeared to require fewer oral SIV exposures to become infected compared to naive controls (9). The current study was designed to include additional control groups to more conclusively determine whether mycobacterial vaccines would predispose infant macaques to SIV infection. Vaccine-induced adaptive immune responses were previously reported (9, 10) and were not assessed in these cohorts. Here, we tested whether mycobacterial vaccines could induce innate immune responses and immune activation. As outlined in Fig. 3, control animals consisted of nine infant macaques that received placebo (phosphate-buffered saline [PBS]) immunization (group C2) and also included the six historical control animals (group C1) from our previous study (9). Similar to the vaccinees in the former study (group D), infant macaques in group E were immunized at birth with mc<sup>2</sup>6435 and mc<sup>2</sup>6439, but instead of receiving heterologous MVA-SIV boosts, the animals received the same mc<sup>2</sup>6435 and mc<sup>2</sup>6439 vaccines (homologous boost) at week 3 by the intradermal (i.d.) route, the current route of BCG vaccination. To exclude other confounding factors, such as SIV antigen expression by *AMtb* vaccines, group F infant macaques were vaccinated with a single dose of mc<sup>2</sup>6208, the parental vaccine strain of mc<sup>2</sup>6435/mc<sup>2</sup>6439 that does not contain SIV expression cassettes. A group of single-dose BCG-vaccinated infants was also included (group G) as a control for vaccine-induced enhanced myeloid cell function and to determine whether any of the effects described here for experimental *AMtb* vaccines may have translational potential for novel TB vaccine in human infants.

Weekly repeated low-dose oral SIV<sub>mac251</sub> challenges were started at week 9 (Fig. 3). On the basis of our observations of persistent immune activation in blood and tissues at 16 to 18 weeks after *AMtb* vaccination of SIV-unexposed infant macaques, we asked whether we could detect activated myeloid cell populations or increased numbers of CCR5-positive CD4<sup>+</sup> T cells (preferred targets for SIV infection) at the time of challenge (week 9).

**Increased function of peripheral blood monocytes/macrophages and mDC of infant macaques vaccinated with *AMtb* or BCG vaccine at the start of oral SIV challenges.** To address this question, we stimulated PBMC that were collected at the time of the start of repeated low-dose oral SIV exposures (week 9) with R848. To

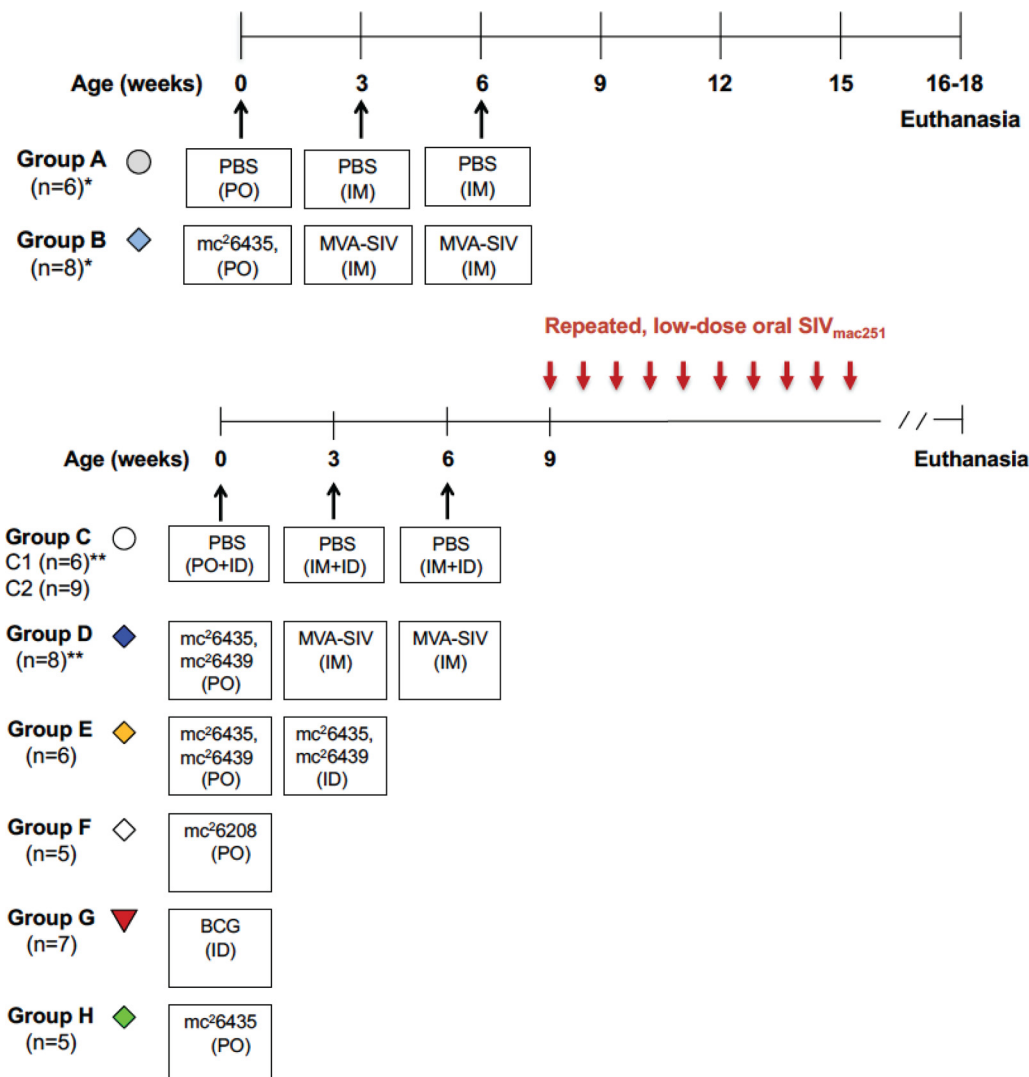
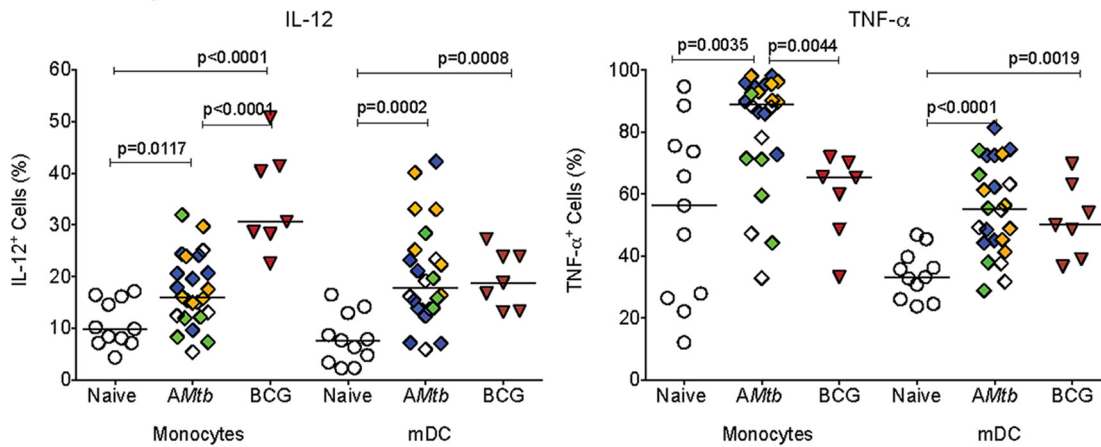


**FIG 3** SIV challenge study outline. The figure shows the times of immunization (indicated by black arrows), the time of oral SIV exposures (red arrows), and lists the vaccine regimens for each of the groups. The number of animals per group is indicated, and each group is assigned a colored symbol. The route of vaccine administration is given in parentheses as follows: PO, per os; IM, intramuscular; ID, intradermal. \*, animal groups have been described in reference 10; \*\*, animal groups have been described in reference 9.

increase our sample size, we included a group of infant macaques that received a single immunization with mc<sup>2</sup>6435 at birth (group H [Fig. 3]); this group was not included in the SIV challenge with analysis, because these infants were challenged with a high dose of SIV<sub>mac251</sub>. Indeed, the frequencies of IL-12-producing monocytes were significantly higher in PBMC from *AMtb*- or BCG-vaccinated infant macaques than from naive control animals, whereas TNF- $\alpha$  responses were increased only in *AMtb*-vaccinated infants (Fig. 4A). Infant macaques vaccinated with *AMtb* or BCG also had significantly higher frequencies of IL-12- or TNF- $\alpha$ -producing mDC than naive controls (Fig. 4A).

We next tested whether these enhanced functional responses of monocytes/macrophages and mDC were associated with systemic immune activation. Week 9 plasma samples were analyzed for a panel of cytokines and chemokines that included several proinflammatory markers. However, none of the cytokines typically associated with inflammation and immune activation, e.g., TNF- $\alpha$ , IL-6, IL-1, and IL-8, were elevated in vaccinated infant macaques. In fact, out of 37 cytokines, chemokines, and growth factors tested, only macrophage chemoattractant 1 (MCP-1) and macrophage inflammatory protein 1 (MIP-1 $\beta$ ) were significantly increased in the plasma of vaccinated

A: TLR Responses



B: Plasma Markers of Monocyte Activation

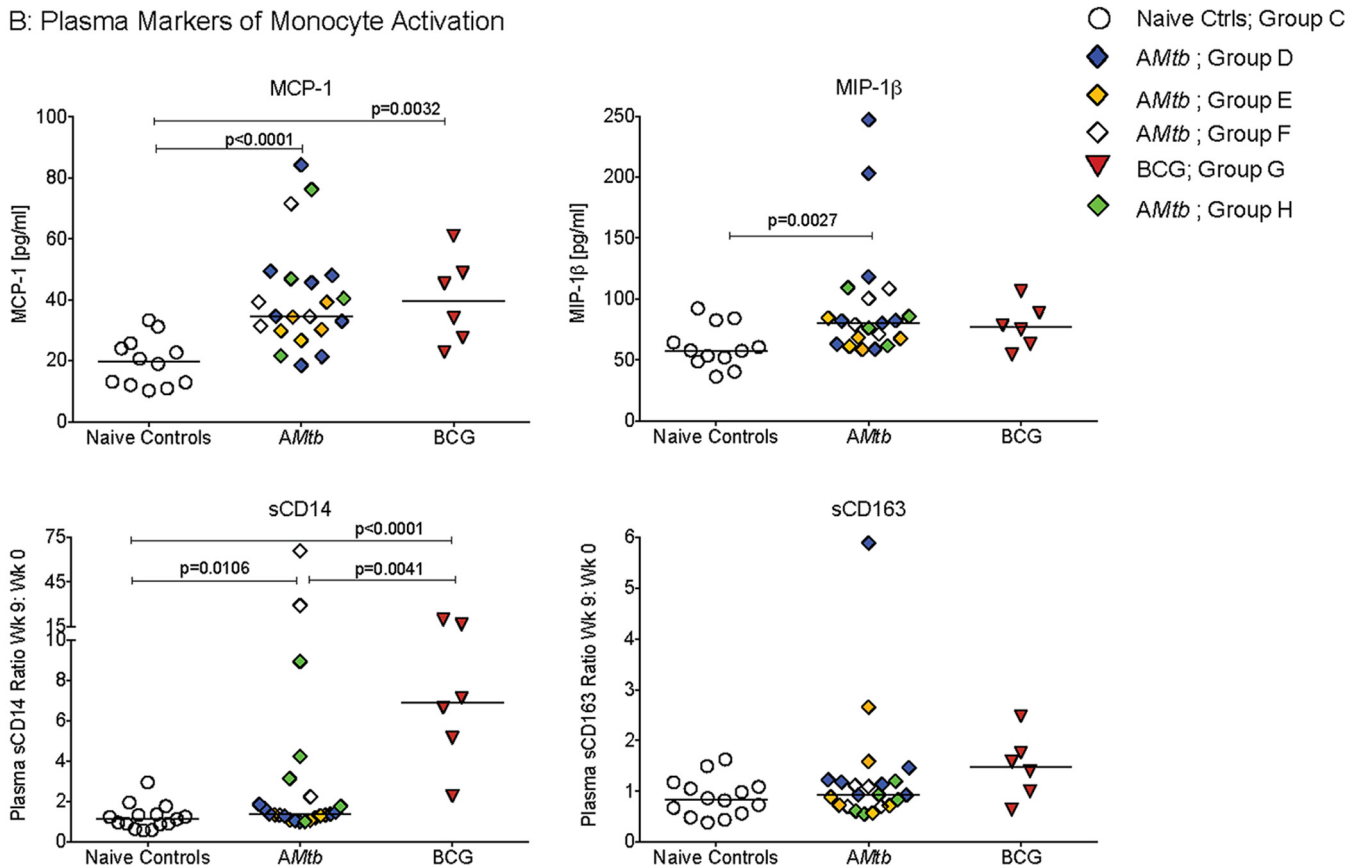


**FIG 4** Vaccine-induced activation of myeloid cells at the time of SIV challenge. (A) Frequencies of IL-12- and TNF- $\alpha$ -producing monocytes/macrophages and mDC in peripheral blood from naive controls, AMtb-vaccinated, and BCG-vaccinated infant macaques at week 9, the time when oral SIV challenges were initiated. (B) Plasma levels of MCP-1 and MIP-1 $\beta$  were measured when the infants were 9 weeks old. The plasma levels of sCD14 and sCD163 are reported as a ratio of the level at week 9 (start of SIV challenge) divided by the level at week 0 (time of immunization). Note that due to the small blood sample volume available from infants, plasma samples were not available for all infants at all time points. Each symbol represents the value for an individual animal with different vaccine groups being identified by their respective colored symbol (Ctrls, controls). Statistically significant differences between the groups are listed as P values and were determined by exact Mann-Whitney test.

animals (Fig. 4B). Both of these cytokines represent markers of monocyte activation. Therefore, we performed further testing for soluble CD14 (sCD14) and sCD163 that are produced by activated monocytes. To account for the large variation in absolute levels between animals and to focus our analysis on vaccination-related changes, we used the ratio of plasma sCD14 and sCD163 levels at week 9 normalized to those at week 0 for

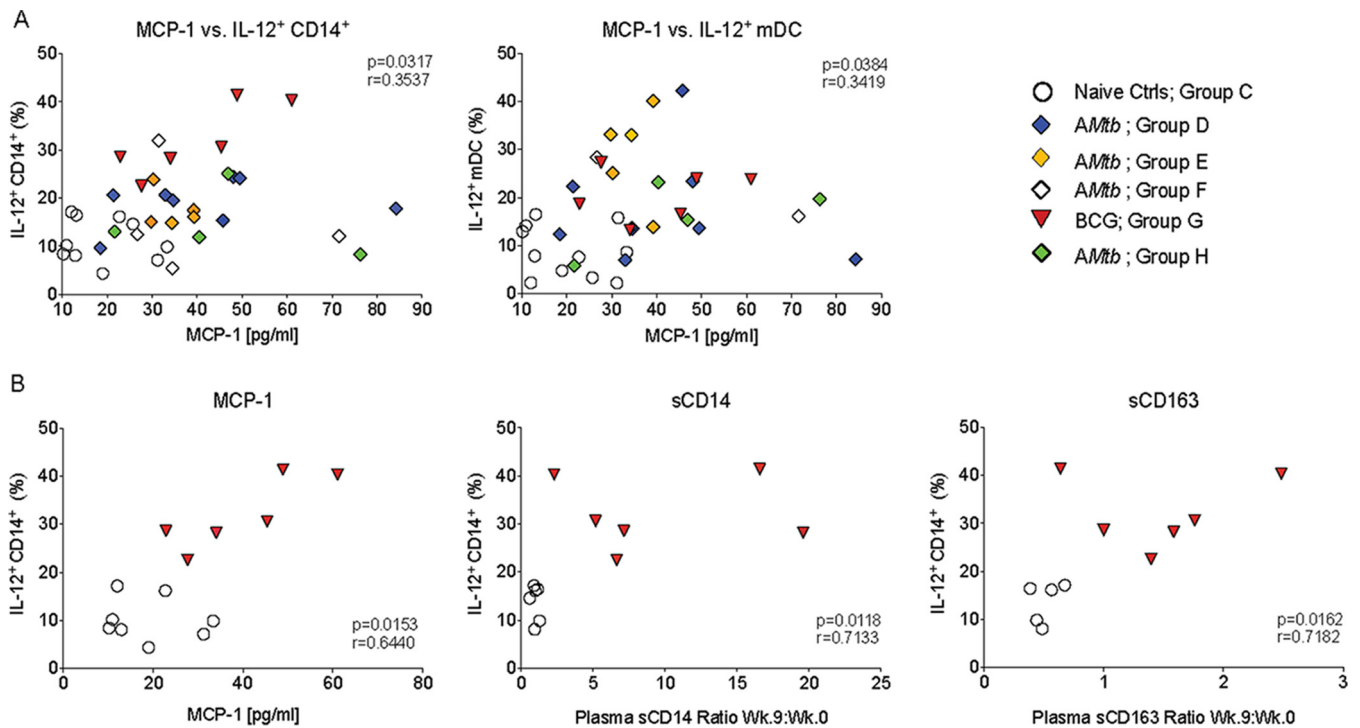


**FIG 5** Correlation between *in vitro* myeloid cell responses and systemic immune activation. (A) Positive correlation between frequencies of IL-12-producing monocytes/macrophages (left) or mDC (right) after *in vitro* R848 stimulation and plasma MCP-1 levels at week 9. (B) Correlation between IL-12-producing monocytes/macrophages and MCP-1, sCD14, and sCD163 including only naive controls and BCG-vaccinated animals in the analysis. Correlations were determined by Spearman rank test. Wk., week.

each animal. Animals vaccinated with *AMtb* or BCG had a significant increase in sCD14 plasma levels, with the increase in sCD14 being significantly higher in BCG-vaccinated compared to *AMtb*-vaccinated infant animals (Fig. 4B). Vaccination was not associated with increased sCD163 plasma levels (Fig. 4B). Consistent with our conclusion that the mycobacterial vaccine component(s), and not MVA boosting or SIV antigen expression, was driving myeloid cell activation, we observed increased functional responses and elevated plasma cytokine levels when we compared each of the *AMtb* vaccine groups separately to the naive control animals at week 9 (see Fig. S1 in the supplemental material).

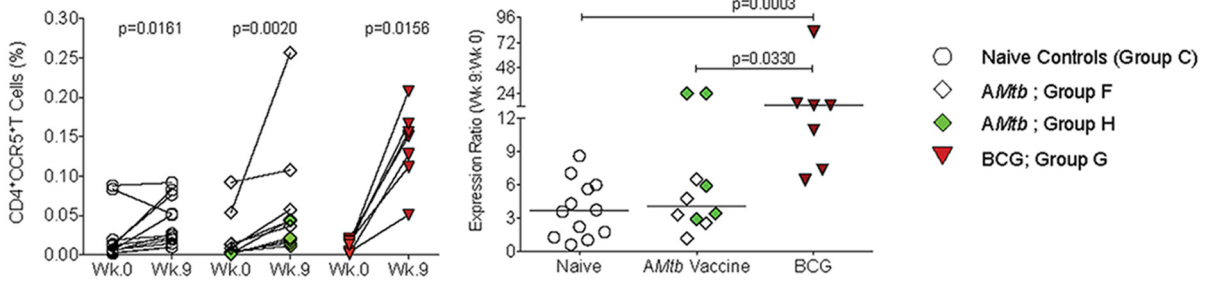
To determine whether the elevated plasma cytokine levels were at least partially due to myeloid cell activation, we tested whether changes in plasma cytokine levels were correlated with functional measurements of myeloid cells at week 9. Indeed, the frequencies of IL-12-producing peripheral blood monocytes/macrophages and mDC were positively correlated with plasma MCP-1 levels (Fig. 5A), but not MIP-1 $\beta$  level (data not shown). This correlation was maintained when we analyzed the relationship between IL-12-positive (IL-12<sup>+</sup>) monocytes/macrophages of BCG-vaccinated animals and naive control animals to plasma MCP-1 (Fig. 5B), but it was not statistically significant when we tested naive controls and *AMtb*-vaccinated infants ( $P = 0.0940$ ) (data not shown). We also observed positive correlations between plasma sCD14 and sCD163 week 9/week 0 ratios and week 9 IL-12<sup>+</sup> monocyte/macrophage frequencies in BCG-vaccinated infants, but not in *AMtb*-vaccinated infants (Fig. 5B).

#### Vaccine-induced CD4<sup>+</sup> T cell activation at the start of oral SIV challenges.

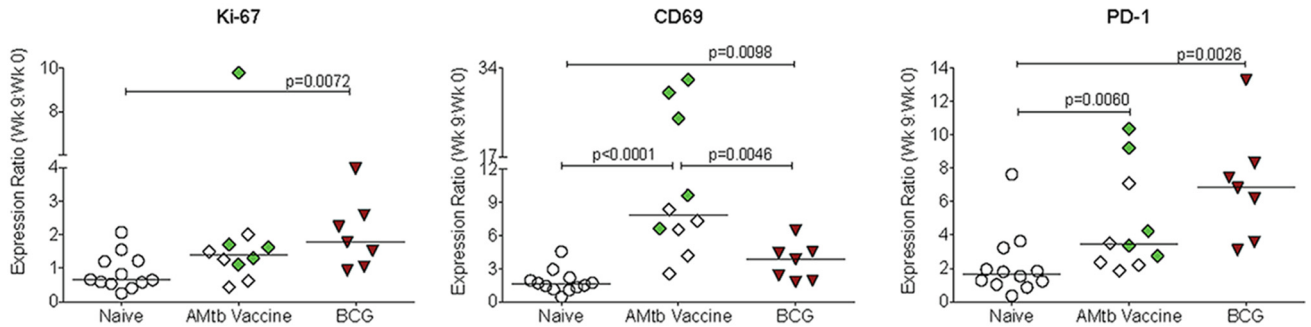
Analysis of longitudinal blood samples showed that all *AMtb*- and BCG-vaccinated infant animals experienced an increase in CD4<sup>+</sup> CCR5<sup>+</sup> T cells after vaccination. However, consistent with the changing ratio of naive to antigen-experienced CD4<sup>+</sup> T cells as part of normal immune development, the frequencies of CCR5<sup>+</sup> CD4<sup>+</sup> T cells increased in all groups between week 0 and week 9 (Fig. 6A). Thus, it was important to distinguish between changes in peripheral blood immune cell populations that reflect normal



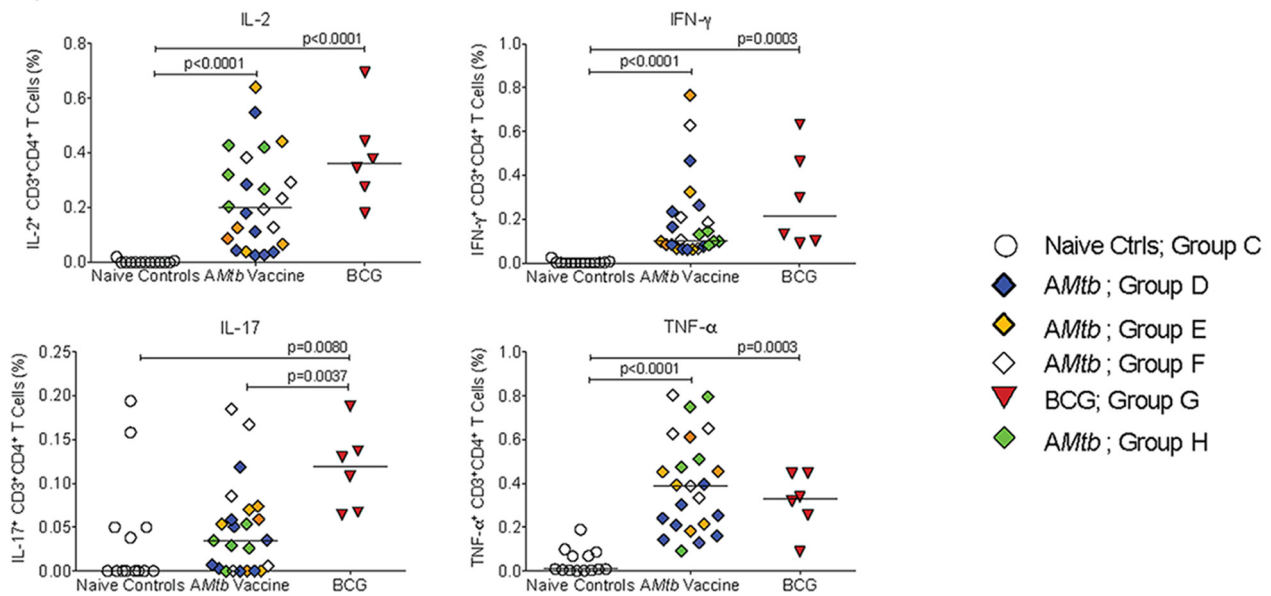
**A: CCR5**



**B: CD4<sup>+</sup> T Cell Activation**



**C: Cytokine Secretion**



**D: CD4<sup>+</sup> T cell activation after DNA-SIV/MVA-SIV vaccination**

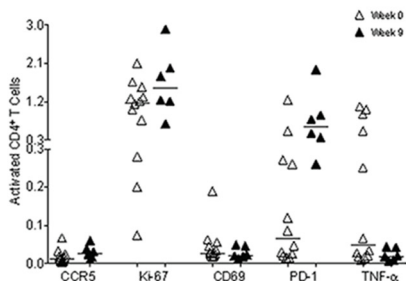


**FIG 6** PBMC CD4<sup>+</sup> T cell activation at week 9. (A) Frequencies of CCR5<sup>+</sup> CD4<sup>+</sup> T cells for individual animals in each group at week 0 (time of immunization) and week 9 (start of SIV challenge); *P* values were determined by Wilcoxon signed-rank test. The right graph shows the ratio of CD4<sup>+</sup> CCR5<sup>+</sup> T cell frequencies at week 9 over week 0. *P* values in this figure were calculated by exact Mann-Whitney test. (B) Between group comparisons in frequencies of CD4<sup>+</sup> T cells

(Continued on next page)

postnatal immune development (38) and vaccine-induced immune activation. Therefore, we report all changes in activated CD4<sup>+</sup> T cell frequencies as ratios of week 9 values compared to week 0 values for each animal. This analysis revealed that BCG-vaccinated infants had significantly higher frequencies of CD4<sup>+</sup> CCR5<sup>+</sup> T cells than naive controls at 9 weeks of age (Fig. 6A). Although CD4<sup>+</sup> CCR5<sup>+</sup> T cells were not increased in *AMtb*-vaccinated infants, vaccine-induced CD4<sup>+</sup> T cell activation was suggested by significantly higher frequencies of CD69<sup>+</sup> and PD-1<sup>+</sup> CD4<sup>+</sup> T cells compared to the naive controls (Fig. 6B). BCG-vaccinated infants showed a significant rise in Ki67<sup>+</sup>, CD69<sup>+</sup>, and in PD-1<sup>+</sup> CD4<sup>+</sup> T cells (Fig. 6B).

Immune activation of CD4<sup>+</sup> T cells was further substantiated by higher levels of endogenous cytokines in *ex vivo* unstimulated CD4<sup>+</sup> T cells from vaccinated animals compared to unvaccinated infant macaques (Fig. 6C). Compared to naive controls, CD4<sup>+</sup> T cells from both *AMtb*- or BCG-vaccinated infants had significantly increased levels of IL-2, gamma interferon (IFN- $\gamma$ ), and TNF- $\alpha$  at week 9, while IL-17A levels were increased only in the BCG-vaccinated infants (Fig. 6C). It should be pointed out that this analysis was performed on *ex vivo* isolated cells without any stimulation and that the measured frequencies of cytokine-producing CD4<sup>+</sup> T cells exceeded those of antigen-specific (both SIV and TB) CD4<sup>+</sup> T cells (9, 10), and thus are consistent with immune activation as opposed to memory responses. Furthermore, an analogous analysis of PBMC samples collected from infant macaques vaccinated with a DNA-SIV prime/MVA-SIV boost regimen did not reveal similar CD4<sup>+</sup> T cell activation (Fig. 6D). These results were confirmed by the statistical significance of separate comparisons of individual *AMtb* vaccine groups to naive control animals (Fig. S2), indicative of mycobacterial vaccine-driven CD4<sup>+</sup> T cell activation.

These combined data show that early vaccination with highly replication-attenuated auxotroph *M. tuberculosis* vaccine strains or with attenuated, but replication-competent BCG, induced activation in myeloid cells and in CD4<sup>+</sup> T cells that was clearly evident at 9 weeks after vaccination, the time of the first oral SIV challenge. While we focused our discussion of mycobacterial-vaccine-induced immune activation on myeloid cells and CD4<sup>+</sup> T cells as the cell types most relevant to SIV acquisition, vaccine-induced immune activation was also observed in CD8<sup>+</sup> T cells and in B cells (Fig. S3), underlining the global nature of systemic immune perturbation, even months after mycobacterial vaccination. Functional differences of CD8<sup>+</sup> T cells and B cells between naive controls and *AMtb*- or BCG-vaccinated infants could not be further explored within the scope of the current study.

**Challenge outcome in *AMtb*- or BCG-vaccinated infant macaques using a repeated low-dose oral SIV exposure model.** Similar to our recent study (9), in which unvaccinated infants had an SIV infection risk per exposure of 0.24, the SIV infection risk per exposure for naive controls was 0.25 in the current study. Thus, 4 of 9 naive controls (44%) became infected after 1 SIV exposure, with 1 animal each requiring 3, 4, 5, or 6 exposures, and 1 animal failing to become persistently infected after 10 oral SIV exposures (not persistently infected [NPI]) (Fig. 7A). In contrast, *AMtb*-vaccinated infants in groups E and F tended to become infected after fewer SIV exposures, with 8 of 11 animals (73%) becoming infected after only one or two exposures (Fig. 7B) and 1 group F animal requiring four exposures. As one infant each in groups E and F remained uninfected after 10 SIV exposures, the SIV infection risk per exposure (0.34) in infant macaques vaccinated with *AMtb* vaccines was lower than in our previous study using the *AMtb*-SIV prime/MVA-SIV

#### FIG 6 Legend (Continued)

expressing Ki-67, CD69, or PD-1 from week 9 to week 0 (exact Mann-Whitney *P* values). (C) Percentages of IL-2-, IFN- $\gamma$ -, IL-17-, and TNF- $\alpha$ -producing CD4<sup>+</sup> T cells in animals from each experimental group at week 9 (exact Mann-Whitney *P* values). (D) Percentages of CCR5-, Ki-67-, CD69-, PD-1-, and TNF- $\alpha$ -positive CD4<sup>+</sup> T cells at week 12 in infant macaques who received an oral DNA-SIV vaccine at weeks 0 and 3 and were vaccinated with MVA-SIV at weeks 6 and 9 by both the intramuscular (i.m.) and sublingual route (DNA expressing SIV<sub>mac239</sub> was encapsulated in cationic liposomes and administered at 3 mg/animal into the mouth; MVA expressing SIV Gag, Pol, and Env was administered at 10<sup>8</sup> PFU by both the i.m. and sublingual route; K. De Paris, unpublished data). No statistically significant differences were noted between week 0 (open triangles) and week 12 (black triangles) values by Wilcoxon signed-rank test.

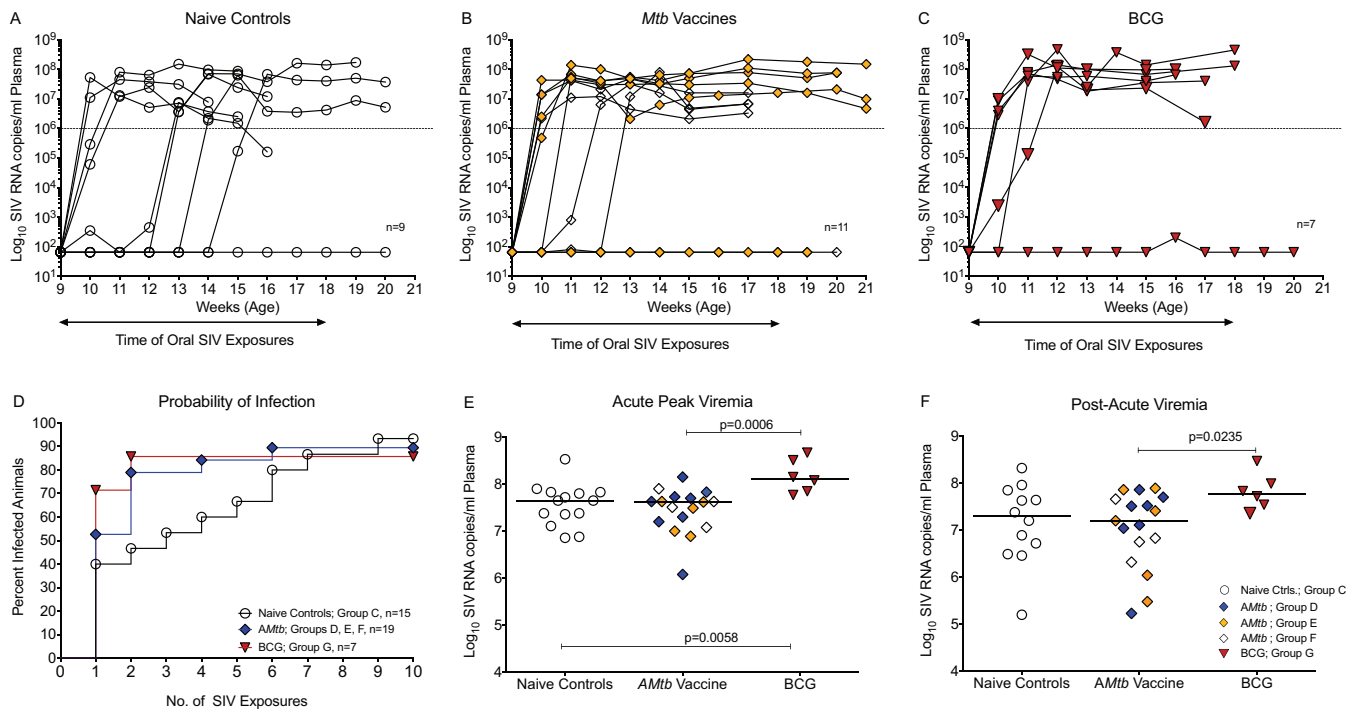


**FIG 7** Challenge outcome using a repeated low-dose oral SIV exposure model. (A) Plasma viremia of naive controls (group C2) after weekly low-dose oral SIV<sub>mac251</sub> exposures, starting at 9 weeks of age. (B) SIV challenge outcome for *AMtb*-vaccinated infants of group E (orange diamonds) and group F (empty diamonds). (C) Challenge outcome of BCG-vaccinated infants. The horizontal axes in panels A to C show the age of the animals. (D) Inverted Kaplan-Meier estimate for the probability of infection per cumulative low-dose SIV exposure for naive controls (groups C1 and C2), *AMtb*-vaccinated infants (groups B, D, E, and F), or BCG-vaccinated infants (group G). The exact log rank test *P* value was not statistically significant. (E and F) Acute and post-acute viremia in naive controls, *AMtb*-, or BCG-vaccinated infants. The *P* values were determined by exact Mann-Whitney test.

boost regimen (exposure risk of 0.5) (9). Similar to *AMtb*, five of seven BCG-vaccinated infants (71%) became infected after a single oral SIV exposure, while one animal required two exposures and one animal remained uninfected for an estimated probability of infection per oral SIV exposure of 0.35 (Fig. 7C).

Given the overall similarity in challenge outcome between the previous (9) and current studies, we combined the animals of both studies to assess the risk of SIV infection. These results translated into a per exposure risk of SIV infection of 0.25 for naive controls (groups A and C) and 0.34 for infant animals receiving any kind of *AMtb* vaccine (groups D, E, and F). As one unvaccinated infant (group C), two *AMtb*-vaccinated infants (groups D to F) and one BCG-vaccinated infant (group G) had to be categorized as NPI, there was only a 1.4-fold increased risk of SIV infection per exposure in vaccinated animals compared to naive control animals. Comparing the *AMtb*-vaccinated animals (*n* = 19) or the BCG-vaccinated animals (*n* = 7) to the control animals (*n* = 15), we did not detect statistically significant differences in the number of SIV exposures until infection (*P* = 0.6 and *P* = 0.8, respectively; Fig. 7D). Yet, descriptively, after only two low-dose oral SIV exposures, 79% of *AMtb*-vaccinated and 88% of BCG-vaccinated infants were infected compared to 47% of naive controls. Furthermore, BCG-vaccinated animals (group G) exhibited significantly higher acute viremia (weeks 1 to 3 postinfection) than *AMtb*-vaccinated animals or naive controls (Fig. 7E), and they tended to have higher viremia during the period after the acute phase of infection (weeks 5 to 7 postinfection; Fig. 7F).

To exclude genetic factors associated with increased susceptibility or resistance to SIV infection or with disease outcome, we determined the tripartite motif-containing protein 5 (TRIM5 $\alpha$ ) and major histocompatibility complex (MHC) class I genotypes of SIV-challenged animals. The TRIM5 $\alpha$  genotypes *TFP/TFP* and *TFP/Cyp* confer resistance to SIV infection, while the genotypes *Q/Q* and *Q/CypA* are associated with increased susceptibility to infection (39, 40). The MHC alleles *Mamu A\*01*, *B\*08*, and *B\*17* alleles

**TABLE 1** MHC class I and *TRIM5α* genotypes

Group and animal no.	Sex <sup>a</sup>	MHC class I type <sup>b</sup>	<i>TRIM5α</i> genotype <sup>c</sup>	Susceptibility score <sup>d</sup>	No. of SIV <sub>mac251</sub> exposures	Age (wk) at euthanasia
Group C <sup>e</sup>						
44586	F	<i>B*01, B*17</i>	<i>Q/CypA</i>	-1	4	16
44618	M	<i>B*01</i>	<i>TFP/TFP</i>	0	3	16
44684	F	<i>A*02, B*08</i>	<i>TFP/TFP</i>	+2	NPI <sup>f</sup>	20
44694	F	<i>B*01</i>	<i>TFP/TFP</i>	0	1	15
44696	M	<i>B*17, B*29</i>	<i>TFP/TFP</i>	+2	1	15
44698	F	<i>B*01, B*08</i>	<i>TFP/TFP</i>	+1	1	14
44718	M	<i>A*01</i>	<i>TFP/Q</i>	+1	6	20
44739	M	Negative <sup>g</sup>	<i>TFP/Q</i>	0	5	20
44746	F	<i>A*01</i>	<i>TFP/Q</i>	+1	1	19
Group D <sup>h</sup>						
Group E						
42903	F	Negative	<i>TFP/Q</i>	0	1	21
42918	M	<i>A*01, B*01</i>	<i>TFP/TFP</i>	+1	NPI	34
42925	F	Negative	<i>TFP/Q</i>	0	1	21
42943	M	<i>A*01</i>	<i>TFP/Q</i>	+1	2	21
42947	F	<i>A*01</i>	<i>TFP/CypA</i>	+2	1	20
42950	M	Negative	<i>TFP/Q</i>	0	1	20
Group F						
44146	F	<i>B*17, B*29</i>	<i>TFP/Q</i>	+1	1	17
44151	F	Negative	<i>TFP/Q</i>	0	2	17
44155	F	<i>B*01, B*17, B*29</i>	<i>TFP/CypA</i>	+1	1	17
44159	F	<i>A*11, B*17, B*29</i>	<i>Q/Q</i>	0	4	17
44160	F	Negative	<i>TFP/Q</i>	0	NPI	41
Group G <sup>i</sup>						
44165	M	<i>A*02, B*01</i>	<i>TFP/TFP</i>	0	NPI	41
44166	M	<i>B*01</i>	<i>TFP/TFP</i>	0	1	16
44169	M	<i>B*01</i>	<i>TFP/TFP</i>	0	1	16
44176	M	Negative	<i>TFP/TFP</i>	+1	2	18
44180	F	<i>A*08</i>	<i>Q/Q</i>	-1	1	18
44186	F	<i>A*02</i>	<i>TFP/TFP</i>	+1	1	17
44195	M	<i>A*08</i>	<i>TFP/Q</i>	0	1	17

<sup>a</sup>F, female; M, male.

<sup>b</sup>The *Mamu A\*01, B\*08, and B\*17* alleles have been associated with better disease outcome, whereas allele *B\*01* is associated with higher viremia.

<sup>c</sup>The *TRIM5α* genotypes *TFP/TFP* and *TFP/CypA* confer resistance to SIV, while the genotypes *Q/Q* and *Q/CypA* are associated with increased susceptibility to infection.

<sup>d</sup>Protective class I alleles and resistant *TRIM5α* alleles (*A\*01, B\*08, TFP/TFP, and TFP/CypA*) were assigned a value of 1. Genotypes associated with increased susceptibility or disease outcome received a score of -1. All other alleles were assigned a score of 0. The susceptibility score represents the sum of all scores for an individual animal (e.g., animal 42376 has MHC 1 + 0 + 1 + 0 and *TRIM5α* of 0 for a score of +2).

<sup>e</sup>In addition, group C includes the six naive control animals (group C1) described by Jensen et al. (9).

<sup>f</sup>NPI, not persistently infected.

<sup>g</sup>Negative, not positive for any of the *Mamu* class I alleles tested (*A\*01, A\*02, A\*08, A\*11, B\*01, B\*03, B\*04, B\*08, B\*17, and B\*29*).

<sup>h</sup>MHC class I and *TRIM5α* genotypes are published in the study by Jensen et al. (9).

<sup>i</sup>Note that group H is not included in this table, because animals received a high-dose SIV challenge and were used for week 9 immune activation measurements, but not for SIV risk calculations. Animals in groups A and B were not exposed to SIV.

have been associated with improved control of viral replication and better disease outcome, whereas allele *B\*01* is associated with higher viremia (41–46). Genotypes could not be evaluated prior to enrollment because animals were assigned to the different groups within 3 days of birth. Animals that required more challenges or were resistant to SIV infection showed no bias toward protective *TRIM5α* alleles or MHC class I alleles, as calculated in the susceptibility score (Table 1). Conversely, animals infected after fewer SIV exposures were not more likely to express alleles associated with greater susceptibility to infection or with reduced control of viremia. Although none of the animals in groups D and E expressed the protective *Mamu A\*01* allele, “MHC protection” refers to the ability to control virus replication better in infected animals; there are no reports, to our knowledge, that conclusively show that the *Mamu A\*01* genotype protects against SIV infection. Similarly, *TRIM5α* alleles have not been associated with resistance to infection with the pathogenic strains SIV<sub>mac239</sub> or SIV<sub>mac251</sub> (47). Therefore,

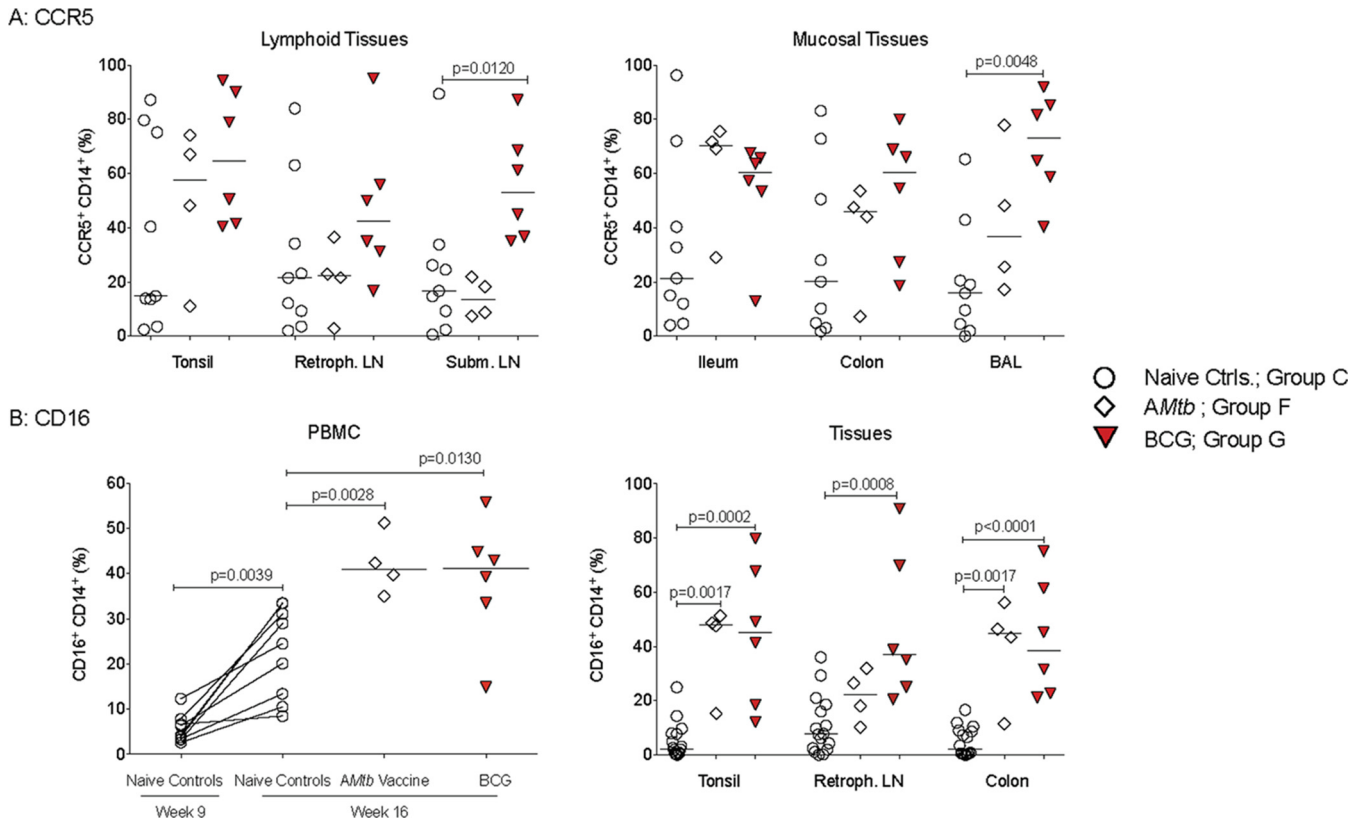


**FIG 8** Myeloid cell activation in blood and tissue samples from vaccinated and SIV-infected infants. (A) Frequencies of CCR5<sup>+</sup> CD14<sup>+</sup> cells in lymphoid and mucosal tissues at the time of euthanasia (Table 1) for animals in group C, F, and G. (B) Frequencies of CD16<sup>+</sup> CD14<sup>+</sup> cells in PBMC and tissues. The *P* values were determined by Wilcoxon signed-rank test for CD16<sup>+</sup> CD14<sup>+</sup> cells in PBMC from naive controls at week 9 compared to week 16 and by exact Mann-Whitney test in all other samples.

we concluded that the genotype of each animal was not a principal cause of enhanced SIV<sub>mac251</sub> acquisition in vaccinated animals.

Collectively, although statistically not significant, the SIV challenge results suggested that infant macaques vaccinated with *AMtb* vaccines or BCG showed a trend toward enhanced SIV acquisition compared to vaccine-naive controls.

**Persistence of vaccine-induced immune activation post-SIV challenge.** Although BCG-vaccinated animals had higher viremia after infection, CD4<sup>+</sup> T cell loss did not differ significantly between these animals, naive controls, and *AMtb*-vaccinated infant animals (data not shown). Histological analysis also revealed no differences in the integrity of the mucosal epithelium between the naive controls and *AMtb*- or BCG-vaccinated groups (data not shown). It is also important to note that mycobacteria could not be recovered from the lung or tracheobronchial lymph nodes of any of the animals at the time of euthanasia. Despite similar clinical outcome, differences in activation of myeloid cells and CD4<sup>+</sup> T cells between naive controls and *AMtb*- or BCG-vaccinated infants were still apparent post-SIV infection. BCG-vaccinated animals had higher frequencies of CCR5<sup>+</sup> monocytes/macrophages in the submandibular lymph nodes and in bronchoalveolar lavage (BAL) fluid than naive control infants did (Fig. 8A). HIV and SIV infections have been associated with increases in CD14<sup>+</sup> CD16<sup>+</sup> cells (48, 49), and while the frequency of activated CD14<sup>+</sup> CD16<sup>+</sup> peripheral blood monocytes in naive controls increased from a median of 4.2% at week 9 to 24.5% after SIV infection (Fig. 8B), even higher frequencies of this cell population were observed in blood and tissues of *AMtb*- and BCG-vaccinated infants. At the time of euthanasia, BCG-vaccinated animals also had higher frequencies of activated CD4<sup>+</sup> T cells in lymphoid tissues than naive controls did (Fig. 9), but differences were not consistently observed in mucosal tissues. In contrast, tissue CD4<sup>+</sup> T cell activation generally did not

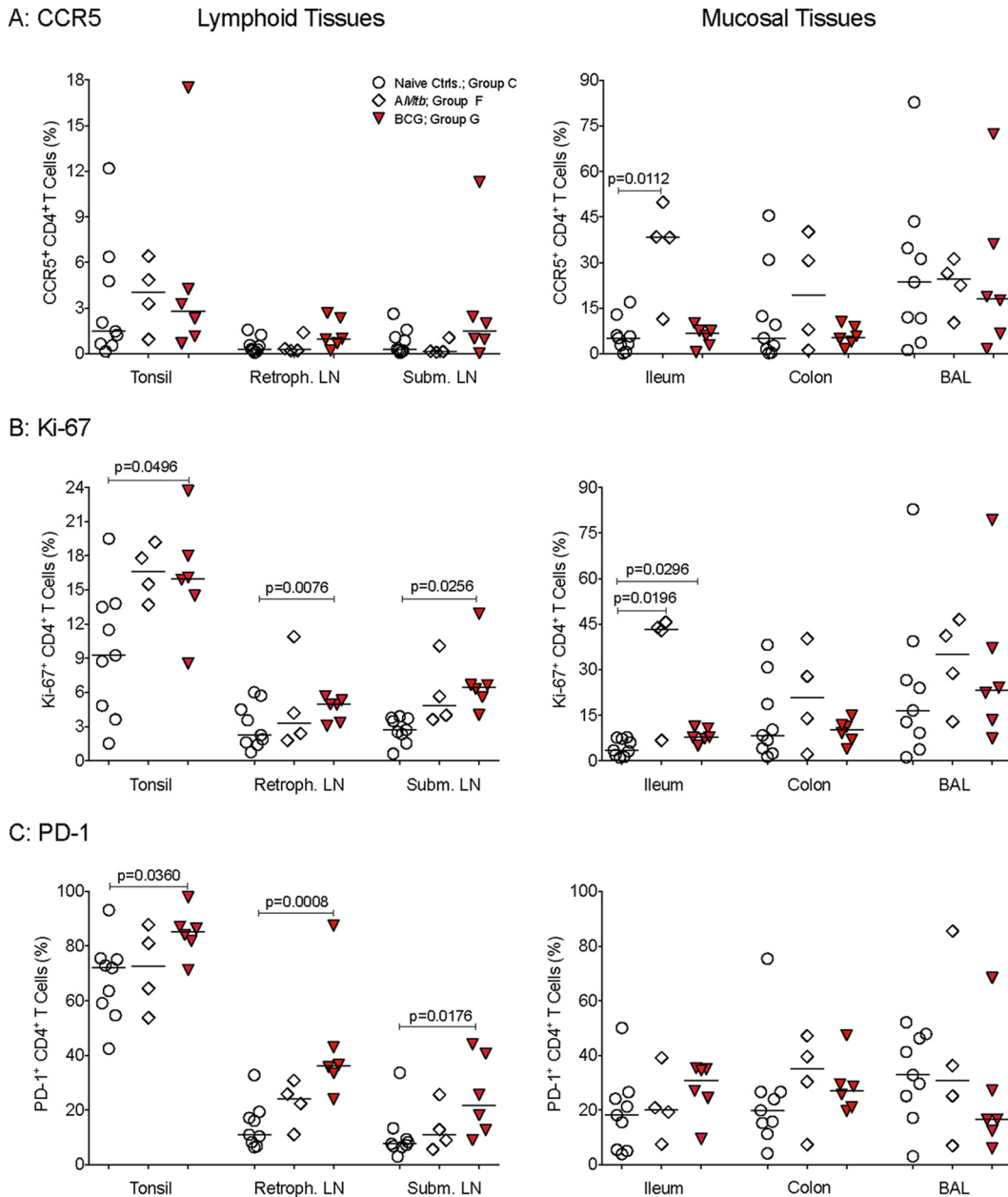
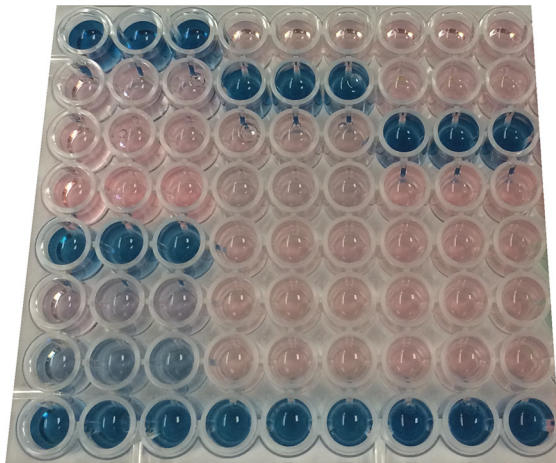


**FIG 9** CD4<sup>+</sup> T cell activation in SIV-infected infant macaques. (A to C) Frequencies of CCR5<sup>+</sup>, Ki-67<sup>+</sup>, and PD-1<sup>+</sup> CD4<sup>+</sup> T cells in lymphoid and mucosal tissues from naive controls and *AMtb*- and BCG-vaccinated animals at the time of euthanasia. The *P* values were determined by exact Mann-Whitney test.

differ significantly between *AMtb*-vaccinated infants and naive controls, except for higher frequencies of CCR5<sup>+</sup> and Ki-67<sup>+</sup> CD4<sup>+</sup> T cells in the ilea of *AMtb*-vaccinated infants (Fig. 9). Similarly, the activation of CD8<sup>+</sup> T cells and B cells was more pronounced in BCG-vaccinated animals (Fig. S4 and S5).

**Differential immune activation of human myeloid cells by BCG and strain mc<sup>2</sup>6435 *in vitro*.** Our data suggested that immune activation of myeloid cell populations might be more pronounced after BCG than *AMtb* vaccination, and thus, we wanted to confirm this effect in human myeloid cells. This direct comparison was also important because the *AMtb* and BCG vaccines were administered at different doses and routes in the infant macaque studies, making a quantitative comparison of immune responses between these two groups difficult. However, the main goal of our studies was to determine whether enhanced myeloid cell function was induced by both

A



	Wells 1-3	Wells 4-6	Wells 7-9
A	TLR2 + HK <i>Mtb</i>	TLR4 + HK <i>Mtb</i>	TLR8 + HK <i>Mtb</i>
B	TLR2 + LPS	TLR4 + LPS	TLR8 + LPS
C	TLR2 + R848	TLR4 + R848	TLR8 + R848
D	TLR2 + water	TLR4 + water	TLR8 + water
E	TLR2 + <i>M. smeg</i>	TLR4 + <i>M. smeg</i>	TLR8 + <i>M. smeg</i>
F	TLR2 + mc <sup>2</sup> 6435	TLR4 + mc <sup>2</sup> 6435	TLR8 + mc <sup>2</sup> 6435
G	TLR2 + BCG	TLR4 + BCG	TLR8 + BCG
H	TLR2 + TNF- $\alpha$	TLR4 + TNF- $\alpha$	TLR8 + TNF- $\alpha$

B

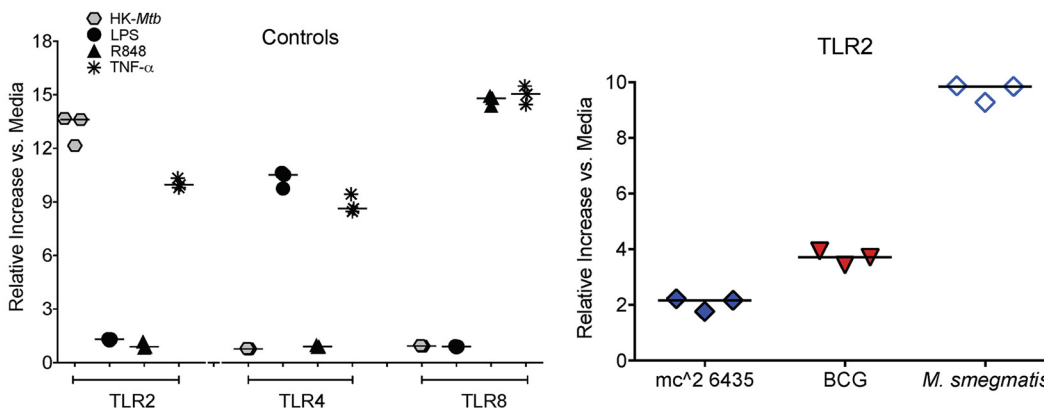


**FIG 10** *Mycobacterium* strains induce TLR2-mediated signaling. (A) Image of the reporter cell line culture plate after 15 h of incubation and the plate template. Blue color is indicative of SEAP secretion and subsequent substrate hydrolysis in culture supernatants. *M. smeg*, *M. smegmatis*. (B, left) Relative increase in NF- $\kappa$ B induction by heat-killed *M. tuberculosis* (HK-*Mtb*), LPS, R848, or TNF- $\alpha$  compared to media in HEK reporter cell lines for TLR2, TLR4, or TLR8. (Right) Relative increase in TLR2-mediated NF- $\kappa$ B activation induced by mc<sup>2</sup>6435, BCG, or *M. smegmatis* mc<sup>2</sup>155. The sample optical density (OD) readings were first corrected for background by subtracting any signal from Null-1 control cells treated with the same stimulants (data not shown). Data points represent the values for three replicates from a representative experiment with median values indicated by the horizontal bar.

vaccine regimens, and thus likely mediated by mycobacteria. To assess for common signaling properties, we first used the HEK-Blue human TLR reporter cell assay to evaluate the TLR2, TLR4, or TLR8 signaling by *M. tuberculosis*-SIV vaccine strain mc<sup>2</sup>6435, BCG, and *Mycobacterium smegmatis* mc<sup>2</sup>155. The highest TLR2 signal was observed after stimulation with *M. smegmatis*, which is thought to be the least immunogenic of the mycobacteria tested (Fig. 10). However, in contrast to the other strains, the replication of *M. smegmatis* is not attenuated, and the higher replication rate may have resulted in stronger signaling. None of the mycobacterial strains induced signaling via TLR4 or TLR8 in a 24-h time period.

We then incubated human PBMC with strain mc<sup>2</sup>6435 or BCG and measured the induction of activation markers and cytokines. Heat-killed mycobacteria (heat-killed *M. tuberculosis* [HK-*Mtb*]) and R848 were included as controls; all responses were corrected for baseline values in unstimulated cultures. Peripheral blood monocytes/macrophages, but not mDC, stimulated with BCG showed higher induction of the costimulatory molecules CD40, CD80, and CD86 than mc<sup>2</sup>6435-stimulated cells did (Fig. 11). Consistent with stronger myeloid cell activation, frequencies of IL-12- and TNF- $\alpha$ -producing monocytes/macrophages and mDC were also higher after BCG stimulation than after mc<sup>2</sup>6435 stimulation (Fig. 12A), and these results were confirmed by increased proin-

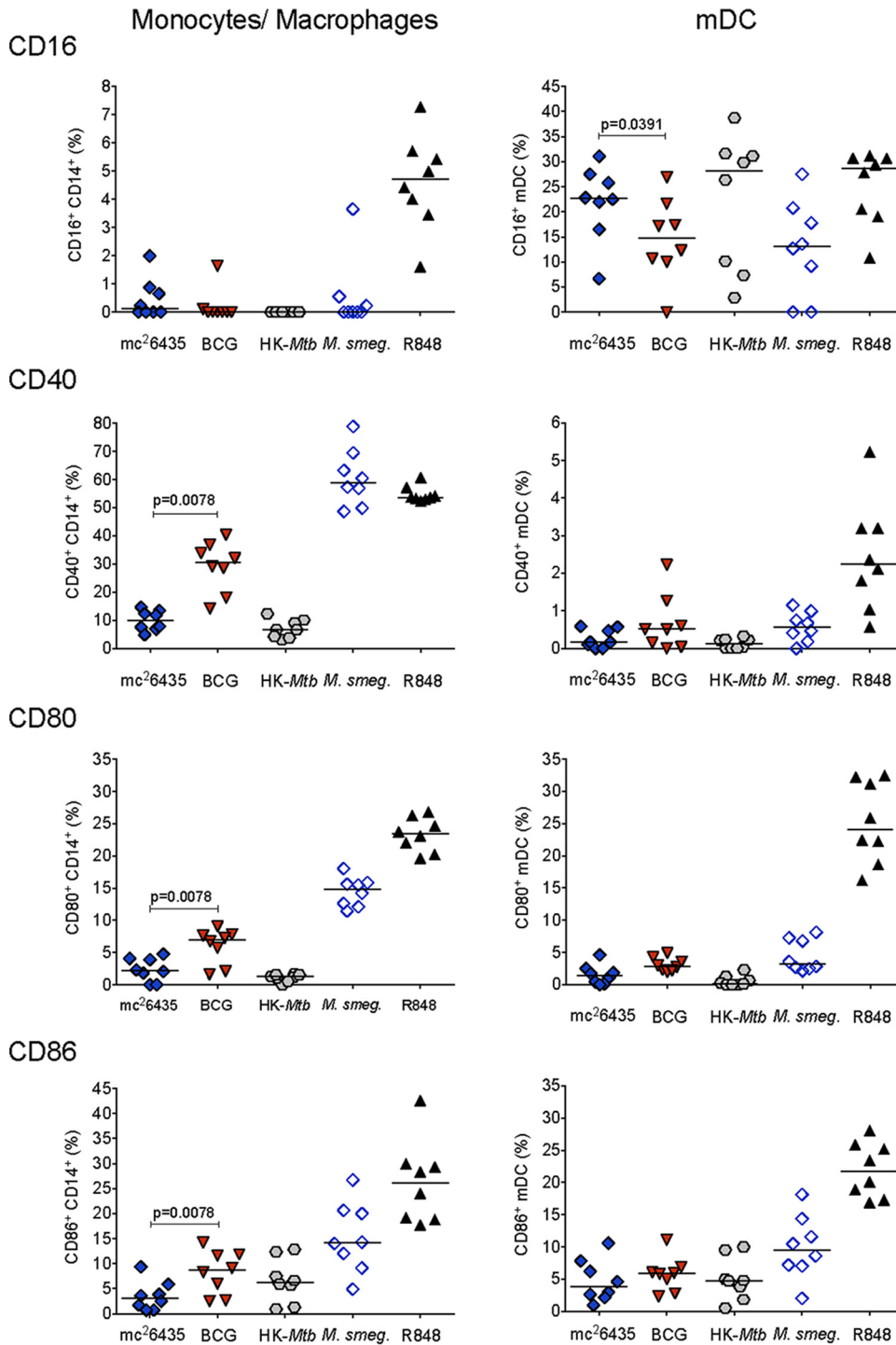


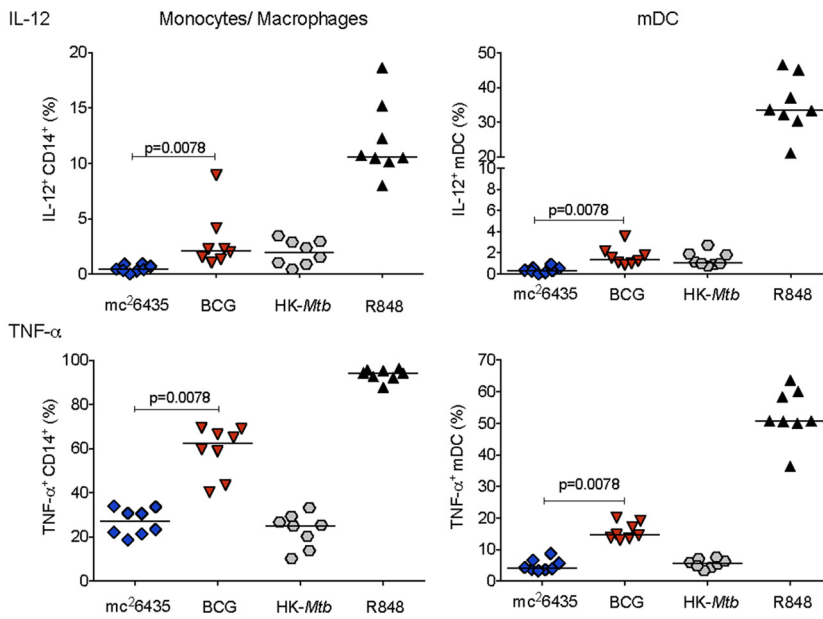
**FIG 11** *In vitro* activation of human monocytes/macrophages by strain mc<sup>2</sup>6435 or BCG. The graphs show the frequencies of CD16-, CD40-, CD80-, or CD86-positive peripheral blood monocytes/macrophages or mDC after a 5-h *in vitro* culture of human PBMC with mc<sup>2</sup>6435, BCG, HK-*Mtb*, or *M. smegmatis* mc<sup>2</sup>155. R848 stimulation served as a positive control. The data for mc<sup>2</sup>6435- and BCG-stimulated samples were compared by exact Mann-Whitney test.

flammatory cytokine secretion into culture supernatants, reiterating the possible impact of vaccine attenuation on cellular activation (Fig. 12B).

These *in vitro* results with adult PBMC confirm that mycobacterial exposure also induces myeloid cell activation in human cells and recapitulates the differences in the degree of activation observed in infant macaques between BCG and our auxotroph



**A: 5-hour Stimulation (Frequencies of cytokine-producing cells)**



**B: 24-hour stimulation (Cytokine Secretion)**

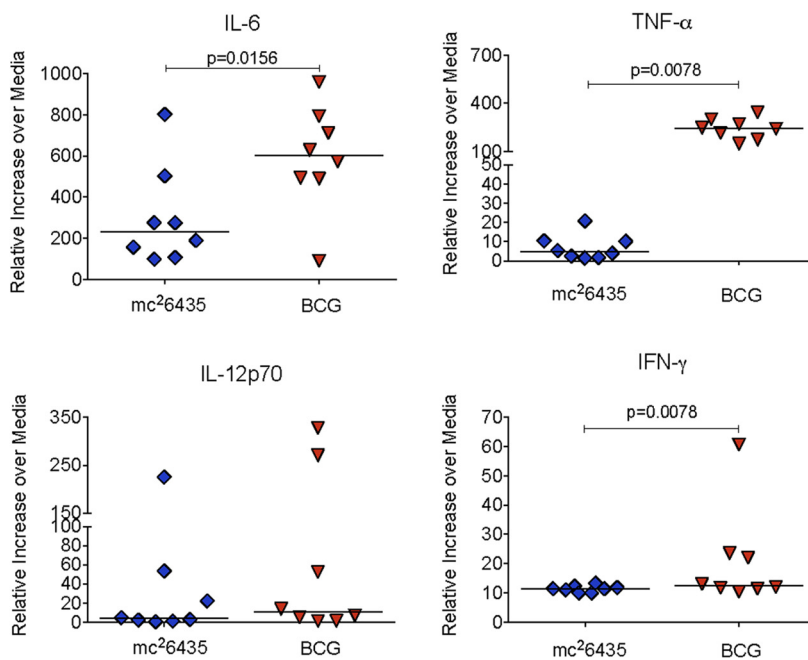


**FIG 12** Cytokine induction in human PMBC. (A) Frequencies of IL-12- or TNF-α-producing myeloid cells were determined by flow cytometry after a 5-h culture with strain mc<sup>2</sup>6435, BCG, HK-Mtb, or R848. (B) Change in IL-6, TNF-α, IL-12p70, or IFN-γ in 24-h culture supernatants of mc<sup>2</sup>6435 or BCG-stimulated human PBMC compared to medium-only cultures. The P values were determined by exact Mann-Whitney test.

vaccine strain mc<sup>2</sup>6435. Further, these experiments were normalized for bacterial dose, suggesting that the *in vivo* studies using different dose and route immunization regimens did not artificially bias immune activation readouts.

**DISCUSSION**

Vaccines to prevent HIV-1 and TB infections are especially needed for vulnerable infant populations in resource-poor countries where limited access to therapies results

in high morbidity and mortality rates. Several new TB vaccine candidates are currently being pursued, many of which take advantage of the potent adjuvant activity of mycobacteria and the nonspecific activation of innate and adaptive immune cells, termed “trained immunity,” which can provide bystander protection against other pathogens (32, 50). These advantages of mycobacterial vaccinations are especially attractive features for pediatric vaccines that need to stimulate the immature infant immune system (51).

Trained immunity was originally described in BCG-vaccinated adults and refers to the persistence of enhanced monocyte function to mycobacterial antigens and heterologous antigens for several months (15). Recently, it was demonstrated that NK cells and T cells of BCG-vaccinated adults can also mediate heterologous immunity (15, 16, 52). While enhanced monocyte function in BCG-vaccinated human adults was associated with NOD2-dependent epigenetic changes (15), the mechanisms mediating trained immunity in NK cells and T cells of BCG-vaccinated adults have not been defined. Multiple mechanisms contribute to heterologous immunity. In fact, the phenomenon of vaccine-induced heterologous immunity has been known for many years and is not limited to BCG, but has also been reported for measles vaccine (31, 53). So far, only live attenuated vaccines have been shown to confer trained immunity (54), suggesting that persistent antigen expression might be essential for its induction. Among the current TB vaccine candidates, the MTBVAC (a mutant of *M. tuberculosis*) and the recombinant BCG vaccine VPM1002 represent live attenuated vaccines with the potential to confer “trained immunity,” and both vaccines have already been shown to exhibit improved safety compared to BCG, while maintaining immunogenicity (55, 56).

Our *AMtb* vaccine strain mc<sup>2</sup>6435 ( $\Delta panCD \Delta leuCD \Delta secA2$ ) is similar in concept to MTBVAC and VPM1002, but it undergoes only limited replication in the mammalian host (8, 57). However, we cannot exclude the possibility that certain bacterial by-products persisted *in vivo* and stimulated innate immune responses. The data of the current study clearly demonstrated that our *AMtb* vaccines enhanced the functional responses of monocytes/macrophages and mDC and that these heightened responses persisted for at least 16 to 18 weeks after a single *AMtb* immunization at birth. These results are consistent with a recent study showing that African infants in Guinea-Bissau had greater responses to various TLR agonists at 4 weeks after BCG vaccination (58). Consistent with findings in BCG-vaccinated adults (16), we also observed vaccine-induced activation of CD4<sup>+</sup> and CD8<sup>+</sup> T cells and of B cells. Our results in infant macaques, which mirrored results from the human pediatric study (58), imply that the phenomenon of mycobacterial-vaccine-induced trained immunity in adults (16) might also be applicable to infants. However, we have not specifically tested for the induction of heterologous immunity and limited cell numbers did not allow us to directly test whether our *AMtb* vaccines induced epigenetic modifications in myeloid cell populations similar to those observed in BCG-vaccinated adults (15). Given our narrow mechanistic understanding of trained immunity in myeloid and other cell populations, additional research is needed to enhance our understanding of the complex interactions between vaccine components, innate immune cell activation, and adaptive immune responses. Such knowledge will be essential to design more-effective and safe vaccine strategies, both for infant and adult populations.

The potent effects of BCG, and similarly *AMtb*, vaccines likely explain the improved immune responses to pediatric vaccines administered to previously BCG-immunized infants (13, 14). Not surprisingly though, the increased functional capacity of myeloid cell populations was associated with persistent immune activation. In comparison to control animals, vaccinated infant macaques had increased levels of MCP-1 in plasma that positively correlated with *in vitro* TLR responses, suggesting that systemic immune activation was driven by myeloid cells, which are target cells for mycobacteria present in live attenuated TB vaccines.

Despite the obvious benefits of improved myeloid function in the context of the maturing infant immune system, persistent immune activation can afford greater susceptibility to HIV infection. Thus, in areas of high HIV prevalence, TB vaccine-induced

immune activation could potentially increase the risk of HIV infection. In fact, it has been reported that BCG vaccination in South African newborns induced an increase in CCR5<sup>+</sup> and in HLA-DR/CD38<sup>+</sup>-expressing CD4<sup>+</sup> T cells (11, 12), raising the question of whether BCG-induced CD4<sup>+</sup> T cell activation might increase the risk of HIV-1 acquisition in the pediatric population. Further, immune activation in the intestine or other sites of virus entry has been associated with increased HIV or SIV acquisition in humans and in nonhuman primates (59–64). This conclusion is supported by our findings that infant macaques vaccinated with *Amtb* or BCG vaccines had increased CD4<sup>+</sup> CCR5<sup>+</sup> T cells in blood and in tissues that serve as presumed entry sites for SIV after oral exposure. Indeed, as in our recent SIV challenge study (9), *Amtb*- or BCG-vaccinated infants in the current study on average required fewer oral SIV exposures to become systemically infected than unvaccinated animals did, and they had a 1.4-fold higher risk of SIV infection per exposure than naive controls of similar age. The differences in per challenge probability of infection did not reach statistical significance between naive controls and *Amtb*- or BCG-vaccinated infant macaques. To conclusively demonstrate a 1.4-fold increased risk of SIV infection would require 100 animals per group to achieve 80% power assuming a 25% per challenge probability of SIV infection in naive controls (<http://www.scharp.org/tools/RLDwebCalc/RLD.php>), a prohibitive study design for multiple reasons. Further, each experimental group included one animal that remained uninfected after 10 exposures, which is not unusual in studies with outbred rhesus macaques, especially protocols like the present one employing low-dose SIV challenge regimens (65, 66). Thus, despite the lack of a formally demonstrated statistically significant difference in acquisition rates between vaccinees and controls, the facts that (i) both *Amtb*- and BCG vaccine-primed infants needed fewer SIV exposures to become infected, (ii) this challenge outcome was observed regardless of vaccine boost, administration route, or known genetic susceptibility factors for SIV, and (iii) compelling statistically significant differences in viremia and in immune activation, the trend toward enhanced SIV acquisition in vaccinated infant macaques may have high biological significance for human infants who receive the BCG vaccine at birth and are at risk for HIV acquisition from breast-feeding.

The importance of vaccine-induced immune activation in relation to HIV infection risk was brought to the forefront by the unexpected results of the STEP HIV vaccine trial (35). Since then, there have been numerous investigations of the mechanisms responsible for increasing HIV susceptibility in STEP vaccine recipients. Some studies have suggested that vaccination with the adenovirus 5 (Ad5) vector activated Ad5-specific memory T cells, increasing the number of target cells for HIV (63, 67–69). However, others have not been able to confirm these results (70, 71). Two recent nonhuman primate studies also suggested that the outcome of SIV challenge is associated with immune activation at the time of challenge. One study showed that PBMC IFN- $\gamma$  enzyme-linked immunosorbent spot assay (ELISPOT) responses inversely correlated with the number of SIV exposures needed to establish infection in adult macaques (72). Another study comparing various vaccine modalities showed that regardless of the vaccine strategy, the number of activated CD4<sup>+</sup> T cells in the rectal mucosa predicted early viremia and risk for rectal SIV infection (73). Both studies established a link between immune activation at the time of challenge and SIV exposure risk, although a statistically significant difference in challenge outcome between the groups was not demonstrated (72, 73). Similarly, in a recent low-dose rectal SIV infection study, animals with higher numbers of Ki67-positive CD4<sup>+</sup> T cells in the colorectal mucosa required fewer SIV exposures to become infected (74). These results are particularly reminiscent of our findings, namely, increased activated CD4<sup>+</sup> T cells at SIV entry sites and SIV infection after fewer exposures in vaccinated infants.

Recent *in vitro* studies provide further evidence that exposure of human CD4<sup>+</sup> T cells to *M. tuberculosis* complex strains including *M. bovis* BCG or *M. tuberculosis* H37Rv derivatives can enhance HIV infection. In the latter study, increased susceptibility was not associated with increased HIV coreceptor expression, but rather with a TLR2-dependent mechanism (75). Although we could confirm that mc<sup>2</sup>6435 signals through

TLR2, it was beyond the scope of our study to test whether *AMtb* or BCG vaccination in infant macaques altered TLR2 expression or TLR2 signaling in CD4<sup>+</sup> T cells. We are planning to explore this mechanism in future studies because TLR2-dependent mechanisms have been implicated in enhanced HIV infectivity (76, 77). The latter study also showed that exposure of human CD4<sup>+</sup> T cells to nonpathogenic *M. smegmatis* mc<sup>2</sup>155 did not result in increased HIV susceptibility (75). Thus, the identification of the specific mycobacterial components that are responsible for immune activation could lead to the design of safer pediatric TB vaccines that do not contain these mycobacterial components (78). Alternatively, genetic factors known to influence TB pathogenesis, such as single nucleotide polymorphisms in CCL2 (chemokine [C-C motif] ligand 2) (79), TLR (80), or cytokine genes (81), could play a role. These are important questions, but they were beyond the scope of the current study that was focused on risk factors for oral SIV acquisition. It is noteworthy that we observed differences between *AMtb* and BCG vaccine-induced immune activation in the *in vivo* studies and could confirm these differences in myeloid cell activation in human PBMC. Mycobacterial strain-specific differences in response magnitudes suggest that the attenuation of the mycobacterial vaccine strains might influence host immune responses, HIV/SIV susceptibility, and disease outcome.

Combined, the data from human studies, adult macaque studies, and the infant macaque studies here, strongly suggest the need to conclusively determine the risk of HIV infection in human infants that are vaccinated with BCG or novel TB vaccine candidates. In areas with a high incidence of TB, even a small increase in the rate of HIV acquisition would have a major impact on pediatric HIV infections. Importantly, a recently published study reported that higher frequencies of activated CD4<sup>+</sup> T cells in BCG-vaccinated human infants from the MVA85A TB vaccine trial had an increased risk for TB disease (82). This is the first report that CD4<sup>+</sup> T cell activation is associated not only with higher HIV infection risk but also with predisposition to TB disease. Considering the high susceptibility of neonates and infants in many resource-poor countries to both HIV and TB, our data reiterate the need to include pediatric populations in clinical trials testing novel TB vaccines and to incorporate immune activation measurements into vaccine safety assessments. Several of our analyses imply that vaccine-induced immune activation was less pronounced in infants vaccinated with the auxotroph *AMtb* vaccine than in those vaccinated with BCG. Therefore, an important goal for future pediatric TB vaccine development should include the design of *AMtb* or BCG vaccine strains with reduced nonspecific immune activation to achieve a balance between potent priming of innate immune responses to induce long-lasting vaccine-induced memory T and B cell responses while avoiding persistent immune activation that could enhance susceptibility to HIV. Concern for such risk might be reduced once (i) new therapeutics, such as long-lasting broadly neutralizing antibodies, become available as treatment options for breast-feeding infants with HIV-infected mothers, (ii) more-frequent HIV testing of mother and child during the breast-feeding period becomes the standard of care, and/or (iii) better adherence of HIV-infected mothers to antiretroviral drug regimens is achieved.

## MATERIALS AND METHODS

**Animals.** Infant rhesus macaques (*Macaca mulatta*) were vaginally delivered by colony dams from the SIV-negative and type D retrovirus-free colony at the California National Primate Research Center (CNPRC; Davis, CA) and reared in the nursery. Infant macaques of the same experimental group were housed in groups of two or three animals, depending on the group size. We strictly adhered to the *Guide for Care and Use of Laboratory Animals* (83) and the standards outlined by the American Association for Accreditation of Laboratory Animal Care; all animal protocols were reviewed and approved by the University of California, Davis Institutional Animal Care and Use Committee prior to study initiation. Animals were randomly assigned to groups and were between 3 and 7 days of age at the first immunization (week 0 in Fig. 3). For all vaccinations and blood draws, animals were immobilized by 10 mg of ketamine-HCl (Parke-Davis, Morris Plains, NJ) per kg of body weight, injected intramuscularly. Complete blood counts (CBC) were performed on each peripheral blood sample by the CNPRC Clinical Laboratory.

**Vaccine strains.** The vaccine strains described in this study were derived from the human-adapted *M. tuberculosis* strain H37Rv as described previously (7, 8, 10). Briefly, the parental H37Rv strain was

engineered with *panCD* and *leuCD* locus deletions to produce a highly attenuated double auxotroph strain mc<sup>2</sup>6206 unable to synthesize the essential nutrients pantothenate and leucine (57). The mc<sup>2</sup>6206 strain was further attenuated by deletion of the *secA2* locus, encoding components of a nonessential secretion system important for bacterial growth, host immune response restriction, and secretion of virulence factors, resulting in strain mc<sup>2</sup>6208. Strain mc<sup>2</sup>6208 was further engineered to coexpress full-length SIVmac239 Gag (mc<sup>2</sup>6435) or Env (mc<sup>2</sup>6439) multimer cassettes that were codon optimized for expression by mycobacteria. MVA-SIV was kindly provided by B. Moss and P. Earl (NIAID, NIH, Bethesda, MD) (84–86).

**Immunizations.** Figure 3 schematically shows the vaccine regimens applied to historical animals (groups A, B, C1, and D) and animals of the current study. Briefly, naive controls (groups A, C1, and C2) were immunized at weeks 0, 3, and 6 with sterile phosphate-buffered saline (PBS) (9). Group B ( $n = 8$ ) and group D animals ( $n = 8$ ) were orally immunized with  $10^9$  CFU each of strains mc<sup>2</sup>6435 and mc<sup>2</sup>6439 at birth before receiving systemic boosts intramuscularly (i.m.) (divided over four injection sites) at weeks 3 and 6 with recombinant modified vaccinia virus Ankara expressing SIVmac239 Gag and Pol (MVA vJH4) and MVA-SIV Env (MVA-SIV; each at  $10^8$  infectious units) as described previously (9). The per os (p.o.) immunizations were done by slowly releasing vaccine with a needleless 1-ml syringe at different sites within the mouth, including the cheek pouches, the sublingual mucosa, and the top of the tongue. Therefore, vaccine uptake could occur locally and after swallowing. In the current study, group E animals ( $n = 6$ ) were primed using the same regimen but received an intradermal (i.d.) boost of a divalent cocktail of  $10^7$  CFU each of strains mc<sup>2</sup>6435 and mc<sup>2</sup>6439 at week 3. We chose to boost group E animals by the i.d. route because the current TB vaccine BCG is administered by this route. Group F infants ( $n = 5$ ) were orally immunized at birth with  $10^9$  CFU of mc<sup>2</sup>6208 without the SIV expression plasmid. Group G animals ( $n = 7$ ) received  $10^5$  CFU of BCG Danish by the i.d. route (Statens Serum Institute, Denmark, Copenhagen) as clinically advised for human newborns. Group H infants received a single p.o. immunization of mc<sup>2</sup>6435 at birth. In order to assess the effects of mycobacterial immunizations alone, animals in groups F, G, and H did not receive booster immunizations.

**SIV challenge.** As described previously (9), low-dose exposures to virulent SIV<sub>mac251</sub> (500 TCID<sub>50</sub>) were administered orally under light anesthesia beginning at week 9 to naive controls (group C) and vaccinated infant macaques (3 or 6 weeks after the last immunization in group D or group E infants, respectively, and 9 weeks after vaccination of infants in groups F and G). The p.o. SIV exposures were performed analogously to the p.o. immunizations in volumes of 1 ml. Animals were challenged weekly until SIV viral RNA levels in plasma indicated persistent infection. We defined persistent infection as 3 or more consecutive weeks of plasma viremia greater than the highest limit of detection over the course of the study ( $\geq 65$  copies of SIV RNA/ml of plasma). Due to the low-dose nature of the challenge model, some animals exhibited episodes of very low transient viremia or measurable viral RNA levels at or below the limit of detection. Animals that failed to become infected after 10 low-dose SIV exposures were right censored for statistical analysis. All animals were monitored for a minimum of 10 weeks after SIV infection and were euthanized before they met clinical criteria established for retrovirus-infected animals (87).

**Sample collection and processing.** EDTA-anticoagulated blood samples were longitudinally collected prior to all interventions throughout the study period. Infant blood sample volumes were based on infant weight and ranged from 0.5 to 3.5 ml per bleed over the course of the study. Plasma was isolated from whole blood by centrifugation and stored in multiple small aliquots at  $-80^{\circ}\text{C}$ . At euthanasia, bronchoalveolar lavage (BAL) fluid samples were collected. Recovered BAL fluid samples were centrifuged to pellet cells which were resuspended in complete RPMI 1640 medium for flow cytometric analysis, while supernatant was aliquoted and stored separately at  $-80^{\circ}\text{C}$ .

At euthanasia, multiple tissues, including tonsil, lymph nodes (LN) (axillary, mesenteric, retropharyngeal, and submandibular), spleen, and intestinal tissues (colon and ileum) were also collected. Tissues were divided into multiple aliquots and (i) formalin fixed/paraffin embedded, (ii) preserved in RNAlater, or (iii) placed in complete media for fresh tissue analysis as previously described (10, 65). Single-cell suspensions for cellular immunity assays were prepared using density gradient centrifugation (whole blood, spleen), gentle homogenization (lymph nodes, tonsil), or collagenase digestion and gradient centrifugation (mucosal tissues) as described previously (10, 65). For the analysis of archived samples, cryopreserved peripheral blood mononuclear cell (PBMC) and tissue cell suspensions from historical animals (9, 10) were quickly thawed at  $37^{\circ}\text{C}$ , immediately washed two times in  $37^{\circ}\text{C}$  serum-free AIM V medium (Thermo Fisher Scientific) supplemented only with antibiotics and allowed to rest overnight at  $37^{\circ}\text{C}$  in 5%  $\text{CO}_2$ . The cells were washed the next day prior to staining for flow cytometric analysis.

**SIV RNA analysis.** Longitudinal plasma samples were used for virological analysis by reverse transcription-PCR (RT-PCR) for SIV RNA essentially as described but with manual RNA extraction for samples with limited volumes (88). Note that limits of detection depended on input plasma volume and ranged from 3 to 65 copies/ml, with a mean of 26 and median of 30. Samples showing transient low viremia followed by SIV RNA-negative time points were retested to confirm the initial PCR results. Data are reported as the number of SIV RNA copy equivalents per milliliter of plasma.

**MHC class I allelic typing.** DNA from cryopreserved splenic cell suspensions was typed for common major histocompatibility complex (MHC) class I variants *Mamu-A\*01*, *-A\*02*, *-A\*08*, *-A\*11*, *-B\*01*, *-B\*03*, *-B\*04*, *-B\*08*, *-B\*17*, and *-B\*29* chosen for their possible roles in restricting SIV infection and/or control of viremia (Table 1). Animals that did not express any of the assayed allelic variants were defined as “negative” (Table 1). Genotyping was completed by the MHC Genotyping Service at the University of Miami Miller School of Medicine using previously reported methods (41, 42, 89–92).

**TRIM5 $\alpha$  genotyping.** The *TRIM5 $\alpha$*  genotype of macaques was determined by sequence analysis of the C-terminal B30.2/SPRY domain of the *TRIM5* gene as described previously (9). The genotypes of

*TRIM5<sup>TFP</sup>*, *TRIM5<sup>Q</sup>*, and *TRIM5<sup>CypA</sup>* were identified, and animals were classified as resistant, intermediate, or sensitive as described previously (39, 40).

**Flow cytometry.** The expression of phenotypic markers, activation markers, and cytokines was evaluated using flow cytometry for T cells, B cells, and monocytes/macrophages in single-cell suspensions from blood and tissues. The cells were stained using rhesus macaque cross-reactive antibodies for phenotype (CD3 [clone SP34-2], CD4 [clone L200], CD8 [clone RP4-T8], CD11c [clone S-HCL-3], CD14 [clone M5E2], CD16 [clone 3G8], CD20 [clone 2H7], and HLA-DR [clone L243]), activation (CCR5 [clone 3A9], CD69 [clone FN50], Ki-67 [clone B56], PD-1 [clone eBioJ105], CD40 [clone 5C3], CD80 [clone L307.4], and CD86 [clone FUN-1]), and cytokine expression (IL-2 [clone MQ1-17H12], TNF- $\alpha$  [clone mab11], IFN- $\gamma$  [clone B27], IL-17 [clone eBio64CAP17], and IL-12 [clone C8.6]) markers alongside a fixable LIVE/DEAD discriminator (Invitrogen). All antibodies were obtained from BD Biosciences, except for PD-1 and IL-17 (eBioscience). The cells were fixed in 1% paraformaldehyde, transferred to PBS, and stored in the dark at 4°C until flow cytometric analysis, which was performed within 24 h. All staining panels were evaluated using fluorescence-minus-one (FMO) controls. Per each sample, 300,000 live, singlet events were acquired on an LSRII instrument. Using FlowJo software (TreeStar, Ashland, OR), cell populations from all staining panels were analyzed by first removing cell debris, multiplet events, and nonviable cells. Monocyte populations were phenotypically defined as CD3<sup>-</sup> CD20<sup>-</sup> CD14<sup>+</sup> HLA-DR<sup>+</sup>, and myeloid dendritic cells were defined as CD3<sup>-</sup> CD14<sup>-</sup> CD20<sup>-</sup> CD11c<sup>+</sup> HLA-DR<sup>+</sup>. Within the lymphocyte gate, T cells were defined as CD3<sup>+</sup> cells and further categorized by expression of either CD4 or CD8 markers to identify classical T cell subsets. B cells were defined within the lymphocyte gate as CD3<sup>-</sup> CD14<sup>-</sup> CD20<sup>+</sup>. Intracellular cytokine responses were reported based on Boolean gating strategies and after subtraction of background responses from unstimulated controls.

**In vitro activation of rhesus macaque blood and tissue myeloid cell populations.** Mononuclear cell suspensions were cultured in complete RPMI 1640 medium in 5-ml fluorescence-activated cell sorting (FACS) tubes with R848 (1  $\mu$ g/ml; InvivoGen) and incubated for 5 h at 37°C/5% CO<sub>2</sub>. At 1 h, brefeldin A (3  $\mu$ g/ml) was added. Unstimulated cells were used in parallel as controls, and any background signal was subtracted from treated cell responses accordingly. Cells were analyzed for activation markers and cytokine production by flow cytometry as described above.

**ELISA/Luminex.** Plasma samples (week 9) were thawed on ice and centrifuged to pellet and remove cellular debris. Plasma samples were then analyzed in duplicate using the nonhuman primate ProcartaPlex 37-plex cytokine/chemokine/growth factor panel (eBioscience) according to the manufacturer's protocol. The assay quantified brain-derived neurotrophic factor (BDNF), B lymphocyte chemoattractant (BLC), eotaxin, fibroblast growth factor 2 (FGF-2), granulocyte colony-stimulating factor (G-CSF), granulocyte-macrophage colony-stimulating factor (GM-CSF), alpha interferon (IFN- $\alpha$ ), IFN- $\gamma$ , interleukin 1 $\beta$  (IL-1 $\beta$ ), IL-10, IL-12p70, IL-13, IL-15, IL-17A, IL-18, IL-1 receptor antagonist (IL-1RA), IL-2, IL-23, IL-4, IL-5, IL-6, IL-7, IL-8, interferon-inducible protein of 10 kDa (IP-10), interferon-inducible T cell alpha chemoattractant (I-TAC), macrophage chemoattractant 1 (MCP-1), monokine induced by gamma interferon (MIG), macrophage inflammatory protein 1 $\alpha$  (MIP-1 $\alpha$ ), MIP-1 $\beta$ , nerve growth factor  $\beta$  (NGF- $\beta$ ), platelet-derived growth factor with two B chains (PDGF-BB), soluble CD40 ligand (sCD40L), stem cell factor (SCF), stromal cell-derived factor 1 $\alpha$  (SDF-1 $\alpha$ ), tumor necrosis factor alpha (TNF- $\alpha$ ), vascular endothelial growth factor A (VEGF-A), and VEGF-D. Plasma levels of sCD14 and sCD163 were measured at birth, on week 9, and at euthanasia by enzyme-linked immunosorbent assay (ELISA) (R&D Systems), according to the manufacturer's protocol.

**Immunohistochemistry.** Immunohistochemistry for myeloperoxidase, Ki-67, and claudin-3, and quantitative image analysis was performed as previously described (93–96).

**M. tuberculosis isolation.** Multiple tissues (lung, bronchial LN, axillary LN, spleen) were snap-frozen and stored at -80°C until shipment to the USDA ARS National Animal Disease Center (Ames, IA) to recover viable mycobacteria using three different culture methods: (i) the fast indicator tube test (MGIT), (ii) Middlebrook 7H12 medium (BacTec), and (iii) solid culture media to determine CFU. Because vaccine strains are auxotrophic, pantothenate- and leucine-supplemented media were used to ensure maximal bacterial recovery. A tissue was considered positive if one of three culture methods yielded mycobacterial growth. *M. tuberculosis* positive-control samples were run in parallel for quality assurance, and the analysis was performed in a blind manner.

**HEK TLR reporter cell assay.** 293HEK-derived cell lines with an NF- $\kappa$ B-inducible secreted embryonic alkaline phosphatase (SEAP) reporter engineered to individually express human Toll-like receptor 2 (TLR2), TLR4, or TLR8 were purchased from InvivoGen (San Diego, CA). The Null-1 parental cell line was used as a control. According to the manufacturer's instructions, the cell lines were passaged twice in growth media (Dulbecco modified Eagle medium [DMEM] supplemented with 10% fetal bovine serum [FBS], 4.5 g/liter glucose, 2 mM L-glutamine, 50 U/ml penicillin, 50  $\mu$ g/ml streptomycin [all from Gibco], and 100  $\mu$ g/ml normocin [InvivoGen]) before the cell lines were expanded under antibiotic selection for plasmid maintenance (1 $\times$  HEK-Blue Selection for TLR2 and TLR4 cell lines and 30  $\mu$ g/ml blasticidin and 100  $\mu$ g/ml zeocin for the TLR8 cell line; all InvivoGen). Cell lines were used for reporter detection experiments between passages 8 and 10, at which time the cells were resuspended in HEK-Blue detection media (InvivoGen) and plated at 50,000 cells/well on 96-well plates with a flat bottom. Human embryonic kidney (HEK) TLR2, TLR4, and TLR8 cells were stimulated in triplicate with previously titrated (i) recombinant human TNF- $\alpha$  (1  $\mu$ g/ml), (ii) heat-killed *M. tuberculosis* (HK-Mtb; 100  $\mu$ g/ml), (iii) ultrapure lipopolysaccharide from *Escherichia coli* K-12 (LPS-EK) (1  $\mu$ g/ml), (iv) R848 (5  $\mu$ g/ml) (items 1 to iv all from InvivoGen), (v) AMtb-SIV vaccine strain mc<sup>2</sup>6435 (multiplicity of infection [MOI] of 5), (vi) *M. bovis* bacillus Calmette-Guérin (MOI of 5), (vii) *M. smegmatis* mc<sup>2</sup>155 (MOI of 5), or (viii) sterile molecular-grade water (Gibco). The plates were incubated at 37°C and 5% CO<sub>2</sub> and monitored longitudinally for 24 h.

TLR-specific signaling was quantified by measuring the colorimetric change induced by HEK-Blue detection medium substrate hydrolysis by SEAP secreted into supernatant by spectrophotometry at 650 nm. The reported values are the colorimetric readings after 15 h of stimulation minus background from Null-1 control cell wells and are representative of longitudinal results through 24 h.

**Human peripheral blood.** The use of human peripheral donor blood for research use was approved by the University of North Carolina at Chapel Hill Institutional Review Board. Blood samples were collected from deidentified healthy adult donors following informed written consent and preserved in EDTA before use within 24 h of collection. The BCG immunization status and purified protein derivative (PPD) reactivity of the blood donors was not disclosed. Mononuclear cells were purified from peripheral blood (PBMC) using density gradient centrifugation over lymphocyte separation medium (MP Biomedical). The cells were resuspended in RPMI 1640 medium (Cellgro) supplemented with 10% heat-inactivated FBS (Gibco) and L-glutamine-penicillin-streptomycin antibiotic cocktail (Sigma) and were used immediately for functional assays.

**In vitro human myeloid cell activation.** PBMC ( $2 \times 10^6$  cells/ml) from eight healthy human adult donors were cultured in complete RPMI 1640 medium in 5-ml FACS tubes with (i) strain mc<sup>2</sup>6435 (MOI of 5), (ii) BCG (MOI of 5), (iii) HK-*Mtb* (5  $\mu$ g/ml; HKMT [InvivoGen]), or (iv) R848 (1  $\mu$ g/ml; InvivoGen) and incubated for 5 h at 37°C and 5% CO<sub>2</sub>, with brefeldin A being added for the last 4 h of culture. Unstimulated cells were used in parallel as controls, and any background signal was subtracted from treated cell responses accordingly. Cells were analyzed for activation markers and cytokine production by flow cytometry as described above.

**In vitro cytokine production by human PBMC.** Human PBMC ( $1 \times 10^6$ ) from eight healthy adult donors were incubated in 1 ml of complete RPMI 1640 medium in 12-well plates with strain mc<sup>2</sup>6435 (MOI of 5), BCG (MOI of 5), or sterile PBS. Culture supernatants were harvested after 18 h, centrifuged, fractionated into small aliquots, and stored at -80°C until ELISA analysis. Each assay was titrated to determine optimal dilutions. Human ELISAs targeting TNF- $\alpha$  and IL-12p70 were purchased from eBioscience, and culture supernatants were assayed at a dilution of 1:10 and undiluted, respectively. Human high-sensitivity IL-6 and IFN- $\gamma$  ELISAs were purchased from R&D Systems and assayed at 1:500 and 1:1 dilutions, respectively. Culture supernatants plus eight dilution standards were assayed in triplicate wells. Reported concentrations have been adjusted first for reference wavelength values and background absorbance from cell-free media before replicates were averaged and multiplied by the relative dilution factor, when applicable.

**Statistical analysis.** Data were analyzed using GraphPad Prism and InStat software (version 6; GraphPad Software, Inc., La Jolla, CA) and SAS version 9.3 (Cary, NC). The probabilities of infection per SIV exposure for naive controls or vaccinated animals were estimated in each group by the number of infected animals divided by the total number of exposures until infection or censoring and were used to estimate the relative risk of infection per exposure. The risk of infection per cumulative number of exposures was estimated using the Kaplan-Meier method and compared between vaccine groups with an exact log rank test. Nonparametric, exact Mann-Whitney tests were used to compare distributions of variables not subject to censoring between two groups. We applied individual exact Mann-Whitney tests because each pairwise comparison was of interest and because the group sizes were small. The exact Wilcoxon signed-rank test was used for within group comparisons of the same variable at two time points. Correlations between two continuous variables were evaluated by Spearman rank test. All statistical tests were two-sided, and *P* values of  $\leq 0.05$  were considered statistically significant. Figures do not show *P* values that did not reach statistical significance, and no adjustment was applied for multiple testing.

## SUPPLEMENTAL MATERIAL

Supplemental material for this article may be found at <https://doi.org/10.1128/CVI.00360-16>.

**TEXT S1**, PDF file, 0.4 MB.

## ACKNOWLEDGMENTS

We are especially grateful to B. Moss and P. Earl for providing us with the MVA-SIV vaccine vectors and to Jeffrey Americo for growth and quality control of the vaccine stocks (Laboratory of Viral Diseases, National Institute of Allergy and Infectious Diseases, NIH, Bethesda, MD). SIV<sub>mac251</sub> was provided by the California National Primate Research Center (CNPRC) Analytical Resource Core. The SIV Gag and Env peptide pools were provided by the NIH AIDS Research and Reference Reagent Program (Division of AIDS, NIAID, NIH). *M. tuberculosis* antigens were provided by BEI Resources. *M. smegmatis* mc<sup>2</sup>155 was kindly provided by Kate Zulauf and Miriam Braunstein, UNC Chapel Hill, NC. We thank J. Lee, K. Jayashankar, Y. Geng, L. Hirst, and Colony Services, Pathology, Veterinary, and Clinical Laboratory staff of the CNPRC. In addition, we thank the University of North Carolina (UNC) Center for AIDS Research (CFAR) and the Department of Microbiology and Immunology at UNC for use of the CFAR Virology, Immunology, and Microbiology Core and Flow Cytometry Core Facilities, respectively. We thank J.

Schmitz and Maggie Conner for assistance with multiplex and ELISAs, and we thank W. J. Bosche, M. Hull, R. Fast, K. Oswald, and R. Shoemaker of the Quantitative Molecular Diagnostics Core of the AIDS and Cancer Virus Program, Frederick National Laboratory for Cancer Research, Frederick, MD, for their help in measuring SIV RNA and DNA in tissue samples. A special thanks to our program officer, I. Rodriguez-Chavez, and to B. Mathieson and J. Patterson for their continued support and advice in these studies.

These studies were supported by NIH grants 1R01 DE019064 (to K.D.P., M.L., and G.F.), T32 AI007419 (Training in Virology), and T32 AI007001-36 (Training in Sexually Transmitted Diseases and AIDS) (to K.J.), by the Louisiana Vaccine Center funded by the Louisiana Board of Regents (P.A.K.), and in part with federal funds from the National Cancer Institute, NIH, under contract HHSN261200800001E. The animal studies at the CNPRC were supported by NIH grants RR00169 from the National Center for Research Resources (NCRR; NIH) and the Office of Research Infrastructure Programs/OD P51 OD011107. Studies at UNC Chapel Hill were supported by the Center for AIDS Research (NIH grant 2 P30 AI050410), by the UNC Flow Cytometry Core that receives support from the Department of Microbiology and Immunology and the NCI Center Core Support Grant P30 CA06086 to the UNC Chapel Hill Lineberger Cancer Center. The MHC Genotyping Service is supported by NIH grant 5R24RR016038 awarded to David Watkins at the University of Miami Miller School of Medicine.

The contents of this publication do not necessarily reflect the views or policies of the U.S. Department of Health and Human Services, nor does mention of trade names, commercial products, or organizations imply endorsement by the U.S. Government.

The funders had no role in the study design, data collection, analysis, or interpretation. The funders also had no influence on the decision for publication of this work.

We declare that we have no conflicts of interest.

## REFERENCES

- Colditz GA, Brewer TF, Berkey CS, Wilson ME, Burdick E, Fineberg HV, Mosteller F. 1994. Efficacy of BCG vaccine in the prevention of tuberculosis. Meta-analysis of the published literature. *JAMA* 271:698–702.
- Rodrigues LC, Diwan VK, Wheeler JG. 1993. Protective effect of BCG against tuberculous meningitis and miliary tuberculosis: a meta-analysis. *Int J Epidemiol* 22:1154–1158. <https://doi.org/10.1093/ije/22.6.1154>.
- Trunz BB, Fine P, Dye C. 2006. Effect of BCG vaccination on childhood tuberculous meningitis and miliary tuberculosis worldwide: a meta-analysis and assessment of cost-effectiveness. *Lancet* 367:1173–1180. [https://doi.org/10.1016/S0140-6736\(06\)68507-3](https://doi.org/10.1016/S0140-6736(06)68507-3).
- Hesseling AC, Marais BJ, Gie RP, Schaaf HS, Fine PE, Godfrey-Faussett P, Beyers N. 2007. The risk of disseminated Bacille Calmette-Guerin (BCG) disease in HIV-infected children. *Vaccine* 25:14–18. <https://doi.org/10.1016/j.vaccine.2006.07.020>.
- Larsen MH, Biermann K, Chen B, Hsu T, Sambandamurthy VK, Lackner AA, Aye PP, Didier P, Huang D, Shao L, Wei H, Letvin NL, Frothingham R, Haynes BF, Chen ZW, Jacobs WR, Jr. 2009. Efficacy and safety of live attenuated persistent and rapidly cleared Mycobacterium tuberculosis vaccine candidates in non-human primates. *Vaccine* 27:4709–4717. <https://doi.org/10.1016/j.vaccine.2009.05.050>.
- Larsen MH, Jacobs WR, Porcelli SA, Kim J, Ranganathan UD, Fennelly GJ. 2010. Balancing safety and immunogenicity in live-attenuated mycobacterial vaccines for use in humans at risk for HIV: response to misleading comments in Ranganathan et al. "Recombinant pro-apoptotic Mycobacterium tuberculosis generates CD8+ T cell responses against human immunodeficiency virus type 1 Env and M. tuberculosis in neonatal mice." *Vaccine* 28:3633–3634. <https://doi.org/10.1016/j.vaccine.2010.03.025>.
- Ranganathan UD, Larsen MH, Kim J, Porcelli SA, Jacobs WR, Jr, Fennelly GJ. 2009. Recombinant pro-apoptotic Mycobacterium tuberculosis generates CD8+ T cell responses against human immunodeficiency virus type 1 Env and M. tuberculosis in neonatal mice. *Vaccine* 28:152–161. <https://doi.org/10.1016/j.vaccine.2009.09.087>.
- Jensen K, Ranganathan UD, Van Rompay KK, Canfield DR, Khan I, Ravindran R, Luciw PA, Jacobs WR, Jr, Fennelly G, Larsen MH, Abel K. 2012. A recombinant attenuated Mycobacterium tuberculosis vaccine strain is safe in immunosuppressed simian immunodeficiency virus-infected infant macaques. *Clin Vaccine Immunol* 19:1170–1181. <https://doi.org/10.1128/CVI.00184-12>.
- Jensen K, Nabi R, Van Rompay KK, Robichaux S, Lifson JD, Piatak M, Jr, Jacobs WR, Jr, Fennelly G, Canfield D, Mollan KR, Hudgens MG, Larsen MH, Amedee AM, Kozlowski PA, De Paris K. 2016. Vaccine-elicited mucosal and systemic antibody responses are associated with reduced simian immunodeficiency viremia in infant rhesus macaques. *J Virol* 90:7285–7302. <https://doi.org/10.1128/JVI.00481-16>.
- Jensen K, Pena MG, Wilson RL, Ranganathan UD, Jacobs WR, Jr, Fennelly G, Larsen M, Van Rompay KK, Kozlowski PA, Abel K. 2013. A neonatal oral Mycobacterium tuberculosis-SIV prime/intramuscular MVA-SIV boost combination vaccine induces both SIV and TB-specific immune responses in infant macaques. *Trials Vaccinol* 2:53–63. <https://doi.org/10.1016/j.trivac.2013.09.005>.
- Hesseling AC, Caldwell J, Cotton MF, Eley BS, Jaspan HB, Jennings K, Marais BJ, Nuttall J, Rabie H, Roux P, Schaaf HS. 2009. BCG vaccination in South African HIV-exposed infants – risks and benefits. *S Afr Med J* 99:88–91.
- Hesseling AK, Passmore J-AS, Gamielidien H, Jones CE, Hanekom W, Sodora DL, Jaspan HB. 2012. BCG vaccination at birth induces non-specific CD4+T cell activation in HIV-exposed South African infants which may increase HIV transmission through breastfeeding, abstr FRLBC04. XIX International AIDS Conference, Washington, DC.
- Libraty DH, Zhang L, Woda M, Acosta LP, Obcena A, Brion JD, Capeding RZ. 2014. Neonatal BCG vaccination is associated with enhanced T-helper 1 immune responses to heterologous infant vaccines. *Trials Vaccinol* 3:1–5. <https://doi.org/10.1016/j.trivac.2013.11.004>.
- Ota MO, Vekemans J, Schlegel-Haueter SE, Fielding K, Sanneh M, Kidd M, Newport MJ, Aaby P, Whittle H, Lambert PH, McAdam KP, Siegrist CA, Marchant A. 2002. Influence of Mycobacterium bovis bacillus Calmette-Guerin on antibody and cytokine responses to human neonatal vaccination. *J Immunol* 168:919–925. <https://doi.org/10.4049/jimmunol.168.2.919>.
- Kleinnijenhuis J, Quintin J, Preijers F, Joosten LA, Iffrim DC, Saeed S, Jacobs C, van Loenhout J, de Jong D, Stunnenberg HG, Xavier RJ, van der Meer JW, van Crevel R, Netea MG. 2012. Bacille Calmette-Guerin induces NOD2-dependent nonspecific protection from reinfection via epigenetic



- reprogramming of monocytes. *Proc Natl Acad Sci U S A* 109: 17537–17542. <https://doi.org/10.1073/pnas.1202870109>.
16. Kleinnijenhuis J, Quintin J, Preijers F, Benn CS, Joosten LA, Jacobs C, van Loenhout J, Xavier RJ, Aaby P, van der Meer JW, van Crevel R, Netea MG. 2014. Long-lasting effects of BCG vaccination on both heterologous Th1/Th17 responses and innate trained immunity. *J Innate Immun* 6:152–158. <https://doi.org/10.1159/000355628>.
  17. Cayabyab MJ, Hovav AH, Hsu T, Krivulka GR, Lifton MA, Gorgone DA, Fennelly GJ, Haynes BF, Jacobs WR, Jr, Letvin NL. 2006. Generation of CD8+ T-cell responses by a recombinant nonpathogenic *Mycobacterium smegmatis* vaccine vector expressing human immunodeficiency virus type 1. *Env. J Virol* 80:1645–1652. <https://doi.org/10.1128/JVI.80.4.1645-1652.2006>.
  18. Hopkins R, Bridgeman A, Bourne C, Mbewe-Mvula A, Sadoff JC, Both GW, Joseph J, Fulkerson J, Hanke T. 2011. Optimizing HIV-1-specific CD8(+) T-cell induction by recombinant BCG in prime-boost regimens with heterologous viral vectors. *Eur J Immunol* 41:3542–3552. <https://doi.org/10.1002/eji.201141962>.
  19. Im EJ, Saubi N, Virgili G, Sander C, Teoh D, Gatell JM, McShane H, Joseph J, Hanke T. 2007. Vaccine platform for prevention of tuberculosis and mother-to-child transmission of human immunodeficiency virus type 1 through breastfeeding. *J Virol* 81:9408–9418. <https://doi.org/10.1128/JVI.00707-07>.
  20. Saubi N, Im EJ, Fernandez-Lloris R, Gil O, Cardona PJ, Gatell JM, Hanke T, Joseph J. 2011. Newborn mice vaccination with BCG.HIVA(2)(2)(2) + MVA.HIVA enhances HIV-1-specific immune responses: influence of age and immunization routes. *Clin Dev Immunol* 2011:516219. <https://doi.org/10.1155/2011/516219>.
  21. Sampson SL, Mansfield KG, Carville A, Magee DM, Quitugua T, Howerth EW, Bloom BR, Hondalus MK. 2011. Extended safety and efficacy studies of a live attenuated double leucine and pantothenate auxotroph of *Mycobacterium tuberculosis* as a vaccine candidate. *Vaccine* 29: 4839–4847. <https://doi.org/10.1016/j.vaccine.2011.04.066>.
  22. Aldovini A, Young RA. 1991. Humoral and cell-mediated immune responses to live recombinant BCG-HIV vaccines. *Nature* 351:479–482. <https://doi.org/10.1038/351479a0>.
  23. Chapman R, Shephard E, Stutz H, Douglass N, Sambandamurthy V, Garcia I, Ryffel B, Jacobs W, Williamson AL. 2012. Priming with a recombinant pantothenate auxotroph of *Mycobacterium bovis* BCG and boosting with MVA elicits HIV-1 Gag specific CD8+ T cells. *PLoS One* 7:e32769. <https://doi.org/10.1371/journal.pone.0032769>.
  24. Chapman R, Stutz H, Jacobs W, Jr, Shephard E, Williamson AL. 2013. Priming with recombinant auxotrophic BCG expressing HIV-1 Gag, RT and Gp120 and boosting with recombinant MVA induces a robust T cell response in mice. *PLoS One* 8:e71601. <https://doi.org/10.1371/journal.pone.0071601>.
  25. Someya K, Cecilia D, Ami Y, Nakasone T, Matsuo K, Burda S, Yamamoto H, Yoshino N, Kaizu M, Ando S, Okuda K, Zolla-Pazner S, Yamazaki S, Yamamoto N, Honda M. 2005. Vaccination of rhesus macaques with recombinant *Mycobacterium bovis* bacillus Calmette-Guerin Env V3 elicits neutralizing antibody-mediated protection against simian-human immunodeficiency virus with a homologous but not a heterologous V3 motif. *J Virol* 79:1452–1462. <https://doi.org/10.1128/JVI.79.3.1452-1462.2005>.
  26. Ami Y, Izumi Y, Matsuo K, Someya K, Kanekiyo M, Horibata S, Yoshino N, Sakai K, Shinohara K, Matsumoto S, Yamada T, Yamazaki S, Yamamoto N, Honda M. 2005. Priming-boosting vaccination with recombinant *Mycobacterium bovis* bacillus Calmette-Guerin and a nonreplicating vaccinia virus recombinant leads to long-lasting and effective immunity. *J Virol* 79:12871–12879. <https://doi.org/10.1128/JVI.79.20.12871-12879.2005>.
  27. Chege GK, Burgers WA, Stutz H, Meyers AE, Chapman R, Kiravu A, Bunjun R, Shephard EG, Jacobs WR, Jr, Rybicki EP, Williamson AL. 2013. Robust immunity to an auxotrophic *Mycobacterium bovis* BCG-VLP prime-boost HIV vaccine candidate in a nonhuman primate model. *J Virol* 87: 5151–5160. <https://doi.org/10.1128/JVI.03178-12>.
  28. Yasutomi Y, Koenig S, Haun SS, Stover CK, Jackson RK, Conard P, Conley AJ, Emini EA, Fuerst TR, Letvin NL. 1993. Immunization with recombinant BCG-SIV elicits SIV-specific cytotoxic T lymphocytes in rhesus monkeys. *J Immunol* 150:3101–3107.
  29. Cayabyab MJ, Koriath-Schmitz B, Sun Y, Carville A, Balachandran H, Miura A, Carlson KR, Buzby AP, Haynes BF, Jacobs WR, Letvin NL. 2009. Recombinant *Mycobacterium bovis* BCG prime-recombinant adenovirus boost vaccination in rhesus monkeys elicits robust polyfunctional simian immunodeficiency virus-specific T-cell responses. *J Virol* 83:5505–5513. <https://doi.org/10.1128/JVI.02544-08>.
  30. Rosario M, Fulkerson J, Soneji S, Parker J, Im EJ, Borthwick N, Bridgeman A, Bourne C, Joseph J, Sadoff JC, Hanke T. 2010. Safety and immunogenicity of novel recombinant BCG and modified vaccinia virus Ankara vaccines in neonate rhesus macaques. *J Virol* 84:7815–7821. <https://doi.org/10.1128/JVI.00726-10>.
  31. Kleinnijenhuis J, van Crevel R, Netea MG. 2015. Trained immunity: consequences for the heterologous effects of BCG vaccination. *Trans R Soc Trop Med Hyg* 109:29–35. <https://doi.org/10.1093/trstmh/tru1168>.
  32. Netea MG, Latz E, Mills KH, O'Neill LA. 2015. Innate immune memory: a paradigm shift in understanding host defense. *Nat Immunol* 16: 675–679. <https://doi.org/10.1038/ni.3178>.
  33. Levy O, Suter EE, Miller RL, Wessels MR. 2006. Unique efficacy of Toll-like receptor 8 agonists in activating human neonatal antigen-presenting cells. *Blood* 108:1284–1290. <https://doi.org/10.1182/blood-2005-12-4821>.
  34. Philbin VJ, Dowling DJ, Gallington LC, Cortes G, Tan Z, Suter EE, Chi KW, Shuckett A, Stoler-Barak L, Tomai M, Miller RL, Mansfield K, Levy O. 2012. Imidazoquinoline Toll-like receptor 8 agonists activate human newborn monocytes and dendritic cells through adenosine-refractory and caspase-1-dependent pathways. *J Allergy Clin Immunol* 130:195–204.e9. <https://doi.org/10.1016/j.jaci.2012.02.042>.
  35. *Lancet*. 2007. STEP study: disappointing, but not a failure. *Lancet* 370: 1665. [https://doi.org/10.1016/S0140-6736\(07\)61702-4](https://doi.org/10.1016/S0140-6736(07)61702-4).
  36. Sekaly RP. 2008. The failed HIV Merck vaccine study: a step back or a launching point for future vaccine development? *J Exp Med* 205:7–12. <https://doi.org/10.1084/jem.20072681>.
  37. Blais ME, Rowland-Jones S. 2009. Lessons from the failure of the adenovector HIV vaccine. *F1000 Biol Rep* 1:50. <https://doi.org/10.3410/B1-50>.
  38. Oxford KL, Dela Pena-Ponce MG, Jensen K, Eberhardt MK, Spinner A, Van Rompay KK, Rigdon J, Mollan KR, Krishnan VV, Hudgens MG, Barry PA, De Paris K. 2015. The interplay between immune maturation, age, chronic viral infection and environment. *Immun Ageing* 12:3. <https://doi.org/10.1186/s12979-015-0030-3>.
  39. Kirmaier A, Wu F, Newman RM, Hall LR, Morgan JS, O'Connor S, Marx PA, Meythaler M, Goldstein S, Buckler-White A, Kaur A, Hirsch VM, Johnson WE. 2010. TRIM5 suppresses cross-species transmission of a primate immunodeficiency virus and selects for emergence of resistant variants in the new species. *PLoS Biol* 8:e1000462. <https://doi.org/10.1371/journal.pbio.1000462>.
  40. Lim SY, Chan T, Gelman RS, Whitney JB, O'Brien KL, Barouch DH, Goldstein DB, Haynes BF, Letvin NL. 2010. Contributions of Mamu-A\*01 status and TRIM5 allele expression, but not CCL3L copy number variation, to the control of SIVmac251 replication in Indian-origin rhesus monkeys. *PLoS Genet* 6:e1000997. <https://doi.org/10.1371/journal.pgen.1000997>.
  41. Giraldo-Vela JP, Rudersdorf R, Chung C, Qi Y, Wallace LT, Bimber B, Borchardt GJ, Fisk DL, Glidden CE, Loffredo JT, Piaskowski SM, Furlott JR, Morales-Martinez JP, Wilson NA, Rehrauer WM, Lifson JD, Carrington M, Watkins DI. 2008. The major histocompatibility complex class II alleles Mamu-DRB1\*1003 and -DRB1\*0306 are enriched in a cohort of simian immunodeficiency virus-infected rhesus macaque elite controllers. *J Virol* 82:859–870. <https://doi.org/10.1128/JVI.01816-07>.
  42. Loffredo JT, Sidney J, Piaskowski S, Szymanski A, Furlott J, Rudersdorf R, Reed J, Peters B, Hickman-Miller HD, Bardet W, Rehrauer WM, O'Connor DH, Wilson NA, Hildebrand WH, Sette A, Watkins DI. 2005. The high frequency Indian rhesus macaque MHC class I molecule, Mamu-B\*01, does not appear to be involved in CD8+ T lymphocyte responses to SIVmac239. *J Immunol* 175:5986–5997. <https://doi.org/10.4049/jimmunol.175.9.5986>.
  43. Evans DT, Knapp LA, Jing P, Mitchen JL, Dykhuizen M, Montefiori DC, Pauza CD, Watkins DI. 1999. Rapid and slow progressors differ by a single MHC class I haplotype in a family of MHC-defined rhesus macaques infected with SIV. *Immunol Lett* 66:53–59. [https://doi.org/10.1016/S0165-2478\(98\)00151-5](https://doi.org/10.1016/S0165-2478(98)00151-5).
  44. Muhl T, Krawczak M, Ten Haaf P, Hunsmann G, Saueremann U. 2002. MHC class I alleles influence set-point viral load and survival time in simian immunodeficiency virus-infected rhesus monkeys. *J Immunol* 169:3438–3446. <https://doi.org/10.4049/jimmunol.169.6.3438>.
  45. Mothe BR, Weinfurter J, Wang C, Rehrauer W, Wilson N, Allen TM, Allison DB, Watkins DI. 2003. Expression of the major histocompatibility complex class I molecule Mamu-A\*01 is associated with control of simian immunodeficiency virus SIVmac239 replication. *J Virol* 77:2736–2740. <https://doi.org/10.1128/JVI.77.4.2736-2740.2003>.

46. O'Connor DH, Mothe BR, Weinfurter JT, Fuenger S, Rehrauer WM, Jing P, Rudersdorf RR, Liebl ME, Krebs K, Vasquez J, Dodds E, Loffredo J, Martin S, McDermott AB, Allen TM, Wang C, Doxiadis GG, Montefiori DC, Hughes A, Burton DR, Allison DB, Wolinsky SM, Bontrop R, Picker LJ, Watkins DI. 2003. Major histocompatibility complex class I alleles associated with slow simian immunodeficiency virus disease progression bind epitopes recognized by dominant acute-phase cytotoxic-T-lymphocyte responses. *J Virol* 77:9029–9040. <https://doi.org/10.1128/JVI.77.16.9029-9040.2003>.
47. Fenizia C, Keele BF, Nichols D, Cornara S, Binello N, Vaccari M, Pegu P, Robert-Guroff M, Ma ZM, Miller CJ, Venzon D, Hirsch V, Franchini G. 2011. TRIM5alpha does not affect simian immunodeficiency virus SIV(mac251) replication in vaccinated or unvaccinated Indian rhesus macaques following intrarectal challenge exposure. *J Virol* 85:12399–12409. <https://doi.org/10.1128/JVI.05707-11>.
48. Ancuta P, Autissier P, Wurcel A, Zaman T, Stone D, Gabuzda D. 2006. CD16+ monocyte-derived macrophages activate resting T cells for HIV infection by producing CCR3 and CCR4 ligands. *J Immunol* 176:5760–5771. <https://doi.org/10.4049/jimmunol.176.10.5760>.
49. Kim WK, Sun Y, Do H, Autissier P, Halpern EF, Piatak M, Jr, Lifson JD, Burdo TH, McGrath MS, Williams K. 2010. Monocyte heterogeneity underlying phenotypic changes in monocytes according to SIV disease stage. *J Leukoc Biol* 87:557–567. <https://doi.org/10.1189/jlb.0209082>.
50. Netea MG, Joosten LA, van der Meer JW, Kullberg BJ, van de Veerdonk FL. 2015. Immune defence against Candida fungal infections. *Nat Rev Immunol* 15:630–642. <https://doi.org/10.1038/nri3897>.
51. Thyssen SM, Aaby P, Benn CS, Fisker AB. 2015. Changes in BCG vaccination policy should consider the effect on child health. *J Infect Dis* 212:1341–1342. <https://doi.org/10.1093/infdis/jiv198>.
52. Kleinnijenhuis J, Quintin J, Preijers F, Joosten LA, Jacobs C, Xavier RJ, van der Meer JW, van Crevel R, Netea MG. 2014. BCG-induced trained immunity in NK cells: role for non-specific protection to infection. *Clin Immunol* 155:213–219. <https://doi.org/10.1016/j.clim.2014.10.005>.
53. Levy O, Levy O. 2015. Ready to benefit from training: heterologous effects of early life immunization. *Trans R Soc Trop Med Hyg* 109:3–4. <https://doi.org/10.1093/trstmh/tru185>.
54. Benn CS, Netea MG, Selin LK, Aaby P. 2013. A small jab - a big effect: nonspecific immunomodulation by vaccines. *Trends Immunol* 34:431–439. <https://doi.org/10.1016/j.it.2013.04.004>.
55. Kaufmann SH, Cotton MF, Eisele B, Gengenbacher M, Grode L, Hesseling AC, Walzl G. 2014. The BCG replacement vaccine VPM1002: from drawing board to clinical trial. *Expert Rev Vaccines* 13:619–630. <https://doi.org/10.1586/14760584.2014.905746>.
56. Arbues A, Aguilo JI, Gonzalo-Asensio J, Marinova D, Uranga S, Puentes E, Fernandez C, Parra A, Cardona PJ, Vilaplana C, Ausina V, Williams A, Clark S, Malaga W, Guilhot C, Gicquel B, Martin C. 2013. Construction, characterization and preclinical evaluation of MTBVAC, the first live-attenuated M. tuberculosis-based vaccine to enter clinical trials. *Vaccine* 31:4867–4873. <https://doi.org/10.1016/j.vaccine.2013.07.051>.
57. Jain P, Hsu T, Arai M, Biermann K, Thaler DS, Nguyen A, Gonzalez PA, Tufariello JM, Kriakov J, Chen B, Larsen MH, Jacobs WR, Jr. 2014. Specialized transduction designed for precise high-throughput unmarked deletions in Mycobacterium tuberculosis. *mBio* 5:e01245-14. <https://doi.org/10.1128/mBio.01245-14>.
58. Jensen KJ, Larsen N, Biering-Sorensen S, Andersen A, Eriksen HB, Monteiro I, Hougaard D, Aaby P, Netea MG, Flanagan KL, Benn CS. 2015. Heterologous immunological effects of early BCG vaccination in low-birth-weight infants in Guinea-Bissau: a randomized-controlled trial. *J Infect Dis* 211:956–967. <https://doi.org/10.1093/infdis/jiu508>.
59. Kahle EM, Bolton M, Hughes JP, Donnell D, Celum C, Lingappa JR, Ronald A, Cohen CR, de Bruyn G, Fong Y, Katabira E, McElrath MJ, Baeten JM, Partners in Prevention HSV/HIV Transmission Study Team. 2015. Plasma cytokine levels and risk of HIV type 1 (HIV-1) transmission and acquisition: a nested case-control study among HIV-1-serodiscordant couples. *J Infect Dis* 211:1451–1460. <https://doi.org/10.1093/infdis/jiu621>.
60. Lehmann S, Relano-Gines A, Resina S, Brillaud E, Casanova D, Vincent C, Hamela C, Poupeau S, Laffont M, Gabelle A, Delaby C, Belongrade M, Arnaud JD, Alvarez MT, Maurel JC, Maurel P, Crozet C. 2014. Systemic delivery of siRNA down regulates brain prion protein and ameliorates neuropathology in prion disorder. *PLoS One* 9:e88797. <https://doi.org/10.1371/journal.pone.0088797>.
61. Naranbhai V, Abdool Karim SS, Altfeld M, Samsunder N, Durgiah R, Sibeko S, Abdool Karim Q, Carr WH, CAPRISA004 TRAPS Team. 2012. Innate immune activation enhances HIV acquisition in women, diminishing the effectiveness of tenofovir microbicide gel. *J Infect Dis* 206:993–1001. <https://doi.org/10.1093/infdis/jis465>.
62. Qureshi H, Genesca M, Fritts L, McChesney MB, Robert-Guroff M, Miller CJ. 2014. Infection with host-range mutant adenovirus 5 suppresses innate immunity and induces systemic CD4+ T cell activation in rhesus macaques. *PLoS One* 9:e106004. <https://doi.org/10.1371/journal.pone.0106004>.
63. Huang Y, Duerr A, Frahm N, Zhang L, Moodie Z, De Rosa S, McElrath MJ, Gilbert PB. 2014. Immune-correlates analysis of an HIV-1 vaccine efficacy trial reveals an association of nonspecific interferon-gamma secretion with increased HIV-1 infection risk: a cohort-based modeling study. *PLoS One* 9:e108631. <https://doi.org/10.1371/journal.pone.0108631>.
64. Hammer SM, Sobieszczyk ME, Janes H, Karuna ST, Mulligan MJ, Grove D, Koblin BA, Buchbinder SP, Keefer MC, Tomaras GD, Frahm N, Hural J, Anude C, Graham BS, Enama ME, Adams E, DeJesus E, Novak RM, Frank I, Bentley C, Ramirez S, Fu R, Koup RA, Mascola JR, Nabel GJ, Montefiori DC, Kublin J, McElrath MJ, Corey L, Gilbert PB, HVTN 505 Study Team. 2013. Efficacy trial of a DNA/rAd5 HIV-1 preventive vaccine. *N Engl J Med* 369:2083–2092. <https://doi.org/10.1056/NEJMoa1310566>.
65. Marthas ML, Van Rompay KK, Abbott Z, Earl P, Buonocore-Buzzelli L, Moss B, Rose NF, Rose JK, Kozlowski PA, Abel K. 2011. Partial efficacy of a VSV-SIV/MVA-SIV vaccine regimen against oral SIV challenge in infant macaques. *Vaccine* 29:3124–3137. <https://doi.org/10.1016/j.vaccine.2011.02.051>.
66. Xiao P, Patterson LJ, Kuate S, Brocca-Cofano E, Thomas MA, Venzon D, Zhao J, DiPasquale J, Fenizia C, Lee EM, Kalisz I, Kalyanaraman VS, Pal R, Montefiori D, Keele BF, Robert-Guroff M. 2012. Replicating adenovirus-simian immunodeficiency virus (SIV) recombinant priming and envelope protein boosting elicits localized, mucosal IgA immunity in rhesus macaques correlated with delayed acquisition following a repeated low-dose rectal SIV(mac251) challenge. *J Virol* 86:4644–4657. <https://doi.org/10.1128/JVI.06812-11>.
67. Sun Y, Bailer RT, Rao SS, Mascola JR, Nabel GJ, Koup RA, Letvin NL. 2009. Systemic and mucosal T-lymphocyte activation induced by recombinant adenovirus vaccines in rhesus monkeys. *J Virol* 83:10596–10604. <https://doi.org/10.1128/JVI.01170-09>.
68. Benlahrech A, Harris J, Meiser A, Papagatsias T, Hornig J, Hayes P, Lieber A, Athanasopoulos T, Bachy V, Csomer E, Daniels R, Fisher K, Gotch F, Seymour L, Logan K, Barbagallo R, Klavinskis L, Dickson G, Patterson S. 2009. Adenovirus vector vaccination induces expansion of memory CD4 T cells with a mucosal homing phenotype that are readily susceptible to HIV-1. *Proc Natl Acad Sci U S A* 106:19940–19945. <https://doi.org/10.1073/pnas.0907898106>.
69. Chakrapurakal G, Onion D, Cobbold M, Mautner V, Moss PA. 2010. Adenovirus vector-specific T cells demonstrate a unique memory phenotype with high proliferative potential and coexpression of CCR5 and integrin alpha4beta7. *AIDS* 24:205–210. <https://doi.org/10.1097/QAD.0b013e3283333addf>.
70. O'Brien KL, Liu J, King SL, Sun YH, Schmitz JE, Lifton MA, Hutnick NA, Betts MR, Dubey SA, Goudsmit J, Shiver JW, Robertson MN, Casimiro DR, Barouch DH. 2009. Adenovirus-specific immunity after immunization with an Ad5 HIV-1 vaccine candidate in humans. *Nat Med* 15:873–875. <https://doi.org/10.1038/nm.1991>.
71. McElrath MJ, De Rosa SC, Moodie Z, Dubey S, Kierstead L, Janes H, Defawe OD, Carter DK, Hural J, Akondy R, Buchbinder SP, Robertson MN, Mehrotra DV, Self SG, Corey L, Shiver JW, Casimiro DR, Step Study Protocol Team. 2008. HIV-1 vaccine-induced immunity in the test-of-concept Step Study: a case-cohort analysis. *Lancet* 372:1894–1905. [https://doi.org/10.1016/S0140-6736\(08\)61592-5](https://doi.org/10.1016/S0140-6736(08)61592-5).
72. Tenbusch M, Ignatius R, Temchura V, Nabi G, Tippler B, Stewart-Jones G, Salazar AM, Saueremann U, Stahl-Hennig C, Uberla K. 2012. Risk of immunodeficiency virus infection may increase with vaccine-induced immune response. *J Virol* 86:10533–10539. <https://doi.org/10.1128/JVI.00796-12>.
73. Carnathan DG, Wetzel KS, Yu J, Lee ST, Johnson BA, Paiardini M, Yan J, Morrow MP, Sardesai NY, Weiner DB, Ertl HC, Silvestri G. 2015. Activated CD4+CCR5+ T cells in the rectum predict increased SIV acquisition in SIVGag/Tat-vaccinated rhesus macaques. *Proc Natl Acad Sci U S A* 112:518–523. <https://doi.org/10.1073/pnas.1407466112>.
74. Sui Y, Lee EM, Wang Y, Hogg A, Frey B, Venzon D, Pal R, Berzofsky JA. 2016. Early SIV dissemination after intrarectal SIVmac251 challenge was associated with proliferating virus-susceptible cells in the colorectum. *J*

- Acquir Immune Defic Syndr 71:353–358. <https://doi.org/10.1097/QAI.0000000000000890>.
75. Thayil SM, Ho YC, Bollinger RC, Blankson JN, Siliciano RF, Karakousis PC, Page KR. 2012. Mycobacterium tuberculosis complex enhances susceptibility of CD4 T cells to HIV through a TLR2-mediated pathway. *PLoS One* 7:e41093. <https://doi.org/10.1371/journal.pone.0041093>.
  76. Ding J, Rapista A, Teleshova N, Mosoyan G, Jarvis GA, Klotman ME, Chang TL. 2010. Neisseria gonorrhoeae enhances HIV-1 infection of primary resting CD4+ T cells through TLR2 activation. *J Immunol* 184: 2814–2824. <https://doi.org/10.4049/jimmunol.0902125>.
  77. Thibault S, Tardif MR, Barat C, Tremblay MJ. 2007. TLR2 signaling renders quiescent naive and memory CD4+ T cells more susceptible to productive infection with X4 and R5 HIV-type 1. *J Immunol* 179:4357–4366. <https://doi.org/10.4049/jimmunol.179.7.4357>.
  78. Skerry C, Klinkenberg LG, Page KR, Karakousis PC. 2016. TLR2-modulating lipoproteins of the Mycobacterium tuberculosis complex enhance the HIV infectivity of CD4+ T cells. *PLoS One* 11:e0147192. <https://doi.org/10.1371/journal.pone.0147192>.
  79. Mishra G, Poojary SS, Raj P, Tiwari PK. 2012. Genetic polymorphisms of CCL2, CCL5, CCR2 and CCR5 genes in Sahariya tribe of North Central India: an association study with pulmonary tuberculosis. *Infect Genet Evol* 12:1120–1127. <https://doi.org/10.1016/j.meegid.2012.03.018>.
  80. Chen Z, Wang W, Liang J, Wang J, Feng S, Zhang G. 2015. Association between Toll-like receptors 9 (TLR9) gene polymorphism and risk of pulmonary tuberculosis: meta-analysis. *BMC Pulm Med* 15:57. <https://doi.org/10.1186/s12890-015-0049-4>.
  81. Bulat-Kardum LJ, Etokebe GE, Lederer P, Balen S, Dembic Z. 2015. Genetic polymorphisms in the Toll-like receptor 10, interleukin (IL)17A and IL17F genes differently affect the risk for tuberculosis in Croatian population. *Scand J Immunol* 82:63–69. <https://doi.org/10.1111/sji.12300>.
  82. Fletcher HA, Snowden MA, Landry B, Rida W, Satti I, Harris SA, Matsumiya M, Tanner R, O'Shea MK, Dheenadhayalan V, Bogardus L, Stockdale L, Marsay L, Chomka A, Harrington-Kandt R, Manjaly-Thomas ZR, Naranbhai V, Stylianou E, Darboe F, Penn-Nicholson A, Nemes E, Hatheril M, Hussey G, Mahomed H, Tameris M, McClain JB, Evans TG, Hanekom WA, Scriba TJ, McShane H. 2016. T-cell activation is an immune correlate of risk in BCG vaccinated infants. *Nat Commun* 7:11290. <https://doi.org/10.1038/ncomms11290>.
  83. National Research Council. 2011. Guide for the care and use of laboratory animals, 8th ed. National Academies Press, Washington, DC.
  84. Earl PL, Wyatt LS, Montefiori DC, Bilska M, Woodward R, Markham PD, Malley JD, Vogel TU, Allen TM, Watkins DI, Miller N, Moss B. 2002. Comparison of vaccine strategies using recombinant env-gag-pol MVA with or without an oligomeric Env protein boost in the SHIV rhesus macaque model. *Virology* 294:270–281. <https://doi.org/10.1006/viro.2001.1345>.
  85. Van Rompay KK, Abel K, Lawson JR, Singh RP, Schmidt KA, Evans T, Earl P, Harvey D, Franchini G, Tartaglia J, Montefiori D, Hattangadi S, Moss B, Marthas ML. 2005. Attenuated poxvirus-based simian immunodeficiency virus (SIV) vaccines given in infancy partially protect infant and juvenile macaques against repeated oral challenge with virulent SIV. *J Acquir Immune Defic Syndr* 38:124–134. <https://doi.org/10.1097/00126334-200502010-00002>.
  86. Winstone N, Wilson AJ, Morrow G, Boggiano C, Chiuchiolo MJ, Lopez M, Kemelman M, Ginsberg AA, Mullen K, Coleman JW, Wu CD, Narpala S, Ouellette I, Dean HJ, Lin F, Sardesai NY, Cassamasa H, McBride D, Felber BK, Pavlakis GN, Schultz A, Hudgens MG, King CR, Zamb TJ, Parks CL, McDermott AB. 2011. Enhanced control of pathogenic simian immunodeficiency virus SIVmac239 replication in macaques immunized with an interleukin-12 plasmid and a DNA prime-viral vector boost vaccine regimen. *J Virol* 85:9578–9587. <https://doi.org/10.1128/JVI.05060-11>.
  87. Van Rompay KK, Singh RP, Brignolo LL, Lawson JR, Schmidt KA, Pahar B, Canfield DR, Tarara RP, Sodora DL, Bischofberger N, Marthas ML. 2004. The clinical benefits of tenofovir for simian immunodeficiency virus-infected macaques are larger than predicted by its effects on standard viral and immunologic parameters. *J Acquir Immune Defic Syndr* 36: 900–914. <https://doi.org/10.1097/00126334-200408010-00003>.
  88. Li H, Wang S, Kong R, Ding W, Lee FH, Parker Z, Kim E, Learn GH, Hahn P, Policicchio B, Brocca-Cofano E, Deleage C, Hao X, Chuang GY, Gorman J, Gardner M, Lewis MG, Hatzioannou T, Santra S, Apetrei C, Pandrea I, Alam SM, Liao HX, Shen X, Tomaras GD, Farzan M, Chertova E, Keele BF, Estes JD, Lifson JD, Doms RW, Montefiori DC, Haynes BF, Sodroski JG, Kwong PD, Hahn BH, Shaw GM. 2016. Envelope residue 375 substitutions in simian-human immunodeficiency viruses enhance CD4 binding and replication in rhesus macaques. *Proc Natl Acad Sci U S A* 113: E3413–E3422. <https://doi.org/10.1073/pnas.1606636113>.
  89. Kaizu M, Borchardt GJ, Glidden CE, Fisk DL, Loffredo JT, Watkins DI, Rehauer WM. 2007. Molecular typing of major histocompatibility complex class I alleles in the Indian rhesus macaque which restrict SIV CD8+ T cell epitopes. *Immunogenetics* 59:693–703. <https://doi.org/10.1007/s00251-007-0233-7>.
  90. Loffredo JT, Friedrich TC, Leon EJ, Stephany JJ, Rodrigues DS, Spencer SP, Bean AT, Beal DR, Burwitz BJ, Rudersdorf RA, Wallace LT, Piaskowski SM, May GE, Sidney J, Gostick E, Wilson NA, Price DA, Kallas EG, Piontkivska H, Hughes AL, Sette A, Watkins DI. 2007. CD8+ T cells from SIV elite controller macaques recognize Mamu-B\*08-bound epitopes and select for widespread viral variation. *PLoS One* 2:e1152. <https://doi.org/10.1371/journal.pone.0001152>.
  91. Loffredo JT, Maxwell J, Qi Y, Glidden CE, Borchardt GJ, Soma T, Bean AT, Beal DR, Wilson NA, Rehauer WM, Lifson JD, Carrington M, Watkins DI. 2007. Mamu-B\*08-positive macaques control simian immunodeficiency virus replication. *J Virol* 81:8827–8832. <https://doi.org/10.1128/JVI.00895-07>.
  92. Yant LJ, Friedrich TC, Johnson RC, May GE, Maness NJ, Enz AM, Lifson JD, O'Connor DH, Carrington M, Watkins DI. 2006. The high-frequency major histocompatibility complex class I allele Mamu-B\*17 is associated with control of simian immunodeficiency virus SIVmac239 replication. *J Virol* 80:5074–5077. <https://doi.org/10.1128/JVI.80.10.5074-5077.2006>.
  93. Canary LA, Vinton CL, Morcock DR, Pierce JB, Estes JD, Brenchley JM, Klatt NR. 2013. Rate of AIDS progression is associated with gastrointestinal dysfunction in simian immunodeficiency virus-infected pigtail macaques. *J Immunol* 190:2959–2965. <https://doi.org/10.4049/jimmunol.1202319>.
  94. Estes JD, Harris LD, Klatt NR, Tabb B, Pittaluga S, Paiardini M, Barclay GR, Smedley J, Pung R, Oliveira KM, Hirsch VM, Silvestri G, Douek DC, Miller CJ, Haase AT, Lifson J, Brenchley JM. 2010. Damaged intestinal epithelial integrity linked to microbial translocation in pathogenic simian immunodeficiency virus infections. *PLoS Pathog* 6:e1001052. <https://doi.org/10.1371/journal.ppat.1001052>.
  95. Somsouk M, Estes JD, Deleage C, Dunham RM, Albright R, Inadomi JM, Martin JN, Deeks SG, McCune JM, Hunt PW. 2015. Gut epithelial barrier and systemic inflammation during chronic HIV infection. *AIDS* 29:43–51. <https://doi.org/10.1097/QAD.0000000000000511>.
  96. Tabb B, Morcock DR, Trubey CM, Quinones OA, Hao XP, Smedley J, Macallister R, Piatak M, Jr, Harris LD, Paiardini M, Silvestri G, Brenchley JM, Alvord WG, Lifson JD, Estes JD. 2013. Reduced inflammation and lymphoid tissue immunopathology in rhesus macaques receiving anti-tumor necrosis factor treatment during primary simian immunodeficiency virus infection. *J Infect Dis* 207:880–892. <https://doi.org/10.1093/infdis/jis643>.